Land uplift due to subsurface fluid injection

Pietro Teatini, Giuseppe Gambolati, Massimiliano Ferronato, A. (tony) Settari, Dale Walters

Accepted Manuscript

Title: Land uplift due to subsurface fluid injection

Authors: Pietro Teatini, Giuseppe Gambolati, Massimiliano Ferronato, A. (Tony) Settari, Dale Walters

Please cite this article as: Teatini, P., Gambolati, G., Ferronato, M., Settari, A.T., Walters, D., Land uplift due to subsurface fluid injection, *Journal of Geodynamics* (2008), doi:10.1016/j.jog.2010.06.001

Land uplift

due to subsurface fluid injection

Pietro Teatini, Giuseppe Gambolati and Massimiliano Ferronato
Department of Mathematical Models and Methods for Scientific Applications
University of Padova, ITALY

A. (Tony) Settari
Department of Chemical and Petroleum Engineering
University of Calgary, CANADA

Dale Walters
TAURUS Reservoir Solutions Ltd., Calgary, CANADA

June 2010, Revised

Corresponding author: Pietro Teatini (teatini@dmsa.unipd.it)

1

1 **Abstract**

2 The subsurface injection of fluid (water, gas, vapour) occurs worldwide for a variety of

3 purposes, e.g. to enhance oil production (EOR), store gas in depleted gas/oil fields,

4 recharge overdrafted aquifer systems (ASR), and mitigate anthropogenic land

5 subsidence. Irrespective of the injection target, some areas have experienced an

6 observed land uplift ranging from a few millimetres to tens of centimetres over a time

7 period of a few months to several years depending on the quantity and spatial

8 distribution of the fluid used, pore pressure increase, geological setting (depth,

9 thickness, and area extent), and hydro-geomechanical properties of the injected

10 formation. The present paper reviews the fundamental geomechanical processes that

11 govern land upheaval due to fluid injection in the subsurface and presents a survey of

12 some interesting examples of anthropogenic uplift measured in the past by the

13 traditional levelling technique and in recent times with the aid of satellite technology.

14 The examples addressed include Long Beach, Santa Clara Valley, and Santa Ana basin,

15 California; Las Vegas Valley, Nevada; Cold Lake and other similar sites, Canada;

16 Tokyo and Osaka, Japan; Taipei, Taiwan; Krechba, Algeria; Upper Palatinate,

17 Germany; Chioggia and Ravenna, Italy.

18 *Keywords*: land uplift; subsurface fluid injection; ground- and satellite-based

19 measurements; hydro-geomechanical properties; case studies

20

1. INTRODUCTION

It is well known that subsurface fluid (groundwater, gas, oil, thermal water) removal induces a land settlement commonly called land subsidence. Magnitude, time of occurrence, and extent of the area involved depend on a large number of factors including the amount of the fluid withdrawn, the pore pressure decline, the depth, volume, and permeability of the pumped formation, and the geomechanical properties of the reservoir and the overburden. For a review of some famous anthropogenically subsiding sites worldwide see Gambolati et al. (2005). The reverse, namely land uplift due to underground fluid injection, is a much less observed and recognized event although the practice of injecting fluids underground is more than a half century old. Injection technology has been advancing continuously since it began to be widely used in the 1950s-1960s to re-inject formation water extracted along with the hydrocarbons, or to dispose of industrial wastes (Donaldson, 1964). The number of injection wells has grown exponentially to the point that EPA (the U.S. Environmental Protection Agency) has identified about 400,000 injection boreholes in the USA alone (USEPA, 2002). The injection of water-based solutions, hydrocarbons, CO_2 or N_2 to enhance oil production (EOR) started in the 1940s and soon became an accepted technique to recover additional oil from reservoirs that were already depleted or waterflooded. Thermal recovery processes, used in reservoirs containing heavy (viscous) oil or bitumen, can also be classified as EOR. There are also examples of water pumped into an oil field to mitigate land subsidence caused by oil production, including, for example, the case of Long Beach, California, where the mitigation programme started in 1958 and was carefully controlled and monitored (Rintoul, 1981).

Land motion related to subsurface fluid injection went unnoticed for a long time in the vast majority of cases. There are a number of reasons for this. First, in most cases

3

45 the disposal of fluids occurred in deserted or sparsely inhabited areas where measuring

46 surface displacements was not a priority, in part due to the large cost of levelling

47 surveys. In other instances uplift was so small that no environmental hazards were

48 created and that no monitoring programme was really needed, or the area involved was

49 quite limited with no damages to the engineered structures and infrastructures reported

50 or even expected. Only in recent times satellite technology has offered a relatively

51 inexpensive, spatially distributed, and accurate methodology to detect ground

52 movements practically worldwide and has revealed anthropogenic uplifts of some

53 interest in terms of magnitude, size of the area involved and time of occurrence. The use

54 of Interferometric Synthetic Aperture Radar (InSAR) techniques has grown rapidly over

55 the last decade, thus facilitating immensely the detection and measurement of rising

56 areas. This is particularly true for surface movements connected with natural

57 fluctuations of the groundwater head and in areas of aquifer storage (ASR), which have

58 been systematically monitored, e.g. Galloway et al. (1998), Amelung et al. (1999),

59 Hoffmann et al. (2001), Watson et al. (2002), Hoffman and Zebker (2003), Schmidt and

60 Bürgmann (2003), Ferretti et al. (2004), Galloway and Hoffmann (2007), Bell et al.

61 (2008). Also surface and borehole tiltmeters have been widely used in recent years to

62 monitor ground heave within relatively small areas.

63   This paper provides a survey of some interesting areas in the world where

64 appreciable heave has been observed mostly as a "by-product" of fluid (water, gas,

65 vapour) injection in geological formations. The mechanics of land rebound is first

66 briefly addressed. The case studies are presented on the basis of the injection purpose,

67 i.e. EOR, ASR, gas storage, land subsidence mitigation, and geomechanical

68 characterization of the geologic formations. The focus is on the magnitude, spatial

69 distribution, and extent of the anthropogenic uplift, with some effort also devoted to

70 describing the geometry of the injected formation, fluid used, depth of disposal,

4

71   duration of the action, and increase of the fluid pore pressure, i.e., the factors controlling

72   the observed displacement field. Finally, two projects on land subsidence mitigation by

73   seawater injection in the Northern Adriatic are described and discussed.

74   **2.   MECHANICS OF LAND UPLIFT DUE TO FLUID INJECTION**

75   Generally speaking, uplift is caused by the migration to the ground surface of the

76   expansion of the geological formation where the fluid is injected. The deformation of

77   the injected porous medium is mainly driven by the in situ pore pressure p and

78   temperature T variations, with the amount of the total displacement mainly controlled

79   by the rock compressibility and thermal expansion coefficient. Based on classical

80   thermo-poro-elastic theory (Coussy, 1995), the partial differential equations governing

81   the rock deformation can be expressed as:

82    $$G\nabla^2\mathbf{u} + (G+\lambda)\nabla\mathrm{div}\mathbf{u} = \alpha\nabla p + \frac{\theta_s}{c_b}\nabla T + \mathbf{b} \tag{1}$$

83   where ∇ and ∇^2 are the gradient and the Laplace operators, respectively, G and λ are

84   the Lamé coefficients generally dependent on the stress path, $\mathbf{u}$ is the displacement

85   vector, α is the Biot coefficient, θ_s is the volumetric thermal expansion coefficient for

86   the solid phase, c_b is the volumetric bulk compressibility, and $\mathbf{b}$ is the vector of body

87   forces. Well-known relationships link the mechanical coefficients in equation (1) to the

88   soil uniaxial vertical compressibility c_M. This is the fundamental geomechanical

89   parameter which basically controls the amount of vertical soil deformation caused by p

90   change and can be acquired from in-situ measurements and lab tests.

91   Different types of fluids can be pumped underground, most commonly water, e.g., to

92   recharge an aquifer system, arrest or mitigate the anthropogenic land subsidence

93   accompanying the development and depletion of aquifers and hydrocarbon fields; but

94   also gas, e.g., steam for EOR, CO_2 for long-term sequestration, or natural gas (methane)

5

95   for gas storage operations. Regardless of the fluid injected, the basic mechanism

96   underlying the geomechanical response is similar with the major differences related to

97   the framework where the operation takes place, i.e. the basin geology, the magnitude of

98   the p and T variations, and therefore the stress path that ultimately controls the

99   deformation. For instance, recharged aquifers are typically shallow, wide, and

100   unconsolidated with the p rise smaller than the previous decline, while gas/oil reservoirs

101   are deeper and more consolidated with a generally lower porosity, permeability and

102   compressibility. In this case the pressure build up can be, at least potentially, much

103   larger than the one experienced by an aquifer. The above factors can generate a very

104   different land surface response in terms of both magnitude and areal distribution

105   according to the specific case at hand.

106   The pore pressure increase in the injected formation may induce new geomechanical

107   processes which are not encountered when fluid is withdrawn. These mechanisms can

108   be more easily understood with the aid of the schematic Mohr representation of the

109   stress state shown in Figure 1 where compressive stresses are taken with the positive

110   sign. When fluid is removed p decreases with respect to the original value ($p < p_0$) and

111   the effective stress, according to Terzaghi's principle, increases. Hence Mohr's circle of

112   Figure 1 moves rightward, i.e. farther from the failure line bounding the envelope of the

113   allowable stress states. By contrast, when fluid is injected p rises and possibly exceeds

114   p_0. In this case the effective stress decreases under the original in situ value with Mohr's

115   circle moving leftward, i.e. toward the failure line. Two failure mechanisms can be

116   experienced: (a) if Mohr's circle touches the envelope line a shear failure may occur; (b)

117   if Mohr's circle crosses the τ-axis a tensile failure takes place. Moreover, a dilation (or

118   dilatancy) phenomenon, i.e. an increase of volumetric strain due to shear, could be

119   induced, thus contributing to the magnitude of the injected formation expansion. Shear

120   dilation accompanies yield and strain weakening with a permanent alteration of the

6

121 fabric of the gas/oil or water bearing stratum through irreversible deformation, grain

122 rearrangement, permeability change and porosity increase, thus causing a potential

123 contribution to a measurable rebound of the land surface (Dusseault and Rothenburg,

124 1988; Settari et al., 1989, 1993). On summary, expansion of the injected formation is

125 primarily caused by a vertical effective stress release due to the pore pressure increase,

126 with the shear stress possibly contributing to deformation through dilation.

127   An additional source of deformation can be of thermal origin. If the temperature of

128 the injected fluids are lower then in-situ temperature, poroelastic and thermal effects on

129 stresses and deformations tend to counteract and may cancel each other. However, in

130 thermal EOR, where the formations involved are usually shallow, both thermal and

131 pressure effects cause expansion and are additive, resulting in appreciable surface

132 heave. According to Wang and Kry (1997) in an analysis of Cyclic Steam Stimulation

133 (CSS) operations conducted in an oil sand at Cold Lake, Alberta, Canada, the pressure

134 effects can dominate because of high injection pressures reached in the CSS process.

135 Conversely, in the Stream Assisted Gravity Drainage (SAGD) process, which uses

136 relatively lower steam injection pressure, experience in modelling (Walters, 2007)

137 shows that the thermal effects can account for 50% or more of the total heave, if the

138 nonlinearity of the geomechanical properties is taken into account.

139   It must be kept in mind that rocks typically exhibit a hysteretic mechanical behaviour

140 with stiffer properties in unloading conditions. For instance, the expansion induced by

141 pore pressure rise in the Northern Adriatic basin is only a third of that of the compaction

142 for a similar pressure decline (Baù et al., 2002; Ferronato et al., 2003).

143   In the survey of uplifted sites that follows it will be shown that anthropogenic land

144 heave can vary from a few millimetres to tens of centimetres depending on the

145 mechanism of deformation (mechanical expansion, dilatancy, thermal deformation) and

146 the several geological and geomechanical factors mentioned above.

7

147   **3.   CASE STUDIES**

148   **3.1.   Injection for EOR**

149   *3.1.1. Cold Lake, Alberta, Canada*

150   Cold Lake is the oldest of the four developed oil sand production areas of northern

151   Alberta, Canada. It is producing from the 15-30 m thick Clearwater sand lying at a

152   depth of about 450 m. The sand is primarily quartz and in the best quality area is quite

153   homogeneous and densely packed; it exhibits dilation when sheared. Above the

154   Clearwater is the Grand Rapids formation consisting of interbedded shale/sand

155   sequences (often containing small gas reservoirs), and the Colorado shale group. A

156   fresh water sandy aquifer at a depth of 100-150 m overlies the Colorado shale. The

157   bitumen viscosity in the Clearwater varies between 50,000 and 100,000 cp at an in-situ

158   temperature close to 13 °C. The area was developed initially by Imperial Oil Ltd. using

159   CSS consisting of cycles of steam injection (30-40 days) at fracturing pressure followed

160   by a production period of several months. Currently, the SAGD process is favoured for

161   new projects.

162   In CSS, the deformations from the pressure cycles (typically between 10 MPa to 2

163   MPa or less) and thermal expansion combine to produce an overall heave of 10-35 cm.

164   Wang and Kry (1997) show the data and simulation results for an area of 3 well "pads"

165   (each consisting of 4 rows of 5 wells) for the period between January 6 and February

166   24, 1989. At the beginning of this period, injection and production was balanced, but

167   due to previous injections, the maximum heave was already about 20 cm, as shown by

168   the baseline on Figure 2a. During the period studied, most of the wells were injecting

169   and this resulted in an additional 5-7 cm of uplift. This magnitude is typical and the

170   heave generally increases with time as the area heats up and accumulates dilation strain.

171   Wong and Lau (2008) confirmed this magnitude by semi-analytical calculations using

8

172   the nucleus of strain concept. Satellite measurements of the Cold Lake project have

173   been described by Stancliffe and van der Kooij (2001). As shown in Figure 2b, large

174   deformation changes can occur over small periods of time (2-3 months). They stated

175   that their best data show that the total deformation can reach 36 cm during a single

176   month.

177   *3.1.2. Shell Peace River, Canada*

178   The Peace River oil sands deposits cover an area of about 47×10^7 m^2 west of the

179   Cold Lake and Athabasca areas. The resource, containing bitumen of viscosity of

180   10,000 to 200,000 cp in a formation 30 m thick buried at a depth of 600 m, has been

181   developed by Shell Canada, using modifications of the CSS technology. Injection takes

182   place at pressures of above 13 MPa (the in-situ vertical stress), thereby producing

183   formation fracturing. An extensive monitoring program, consisting of microseismic,

184   surface time-lapse seismic, time-lapse 3D vertical seismic profiles, surface tiltmeters

185   and InSAR, was implemented to better understand the production mechanisms, and

186   determine the reservoir volume change. In particular, tiltmeter data were used

187   extensively. The data interpretation indicated a similar magnitude of heave as that as

188   Cold Lake, as shown in Figure 3 (Du et al., 2005). McGillivray et al. (2006) reported

189   that during the first year (Oct. 2002-Oct. 2003), the reservoir volume increased by

190   400,000 m^3.

191   *3.1.4. Athabasca oil sands, Canada*

192   The Underground Test Facility (UTF), located in the Athabasca area, was the first

193   field scale project designed to test the SAGD recovery method for oil sands. UTF

194   operates at a depth of about 140 m. During the first phase, started in 1984, 3 pairs of

195   short horizontal wells were drilled from an underground tunnel accessed by a vertical

196   shaft. The second phase followed with 3 pairs of long (500 m) horizontal wells from

9

197   which commercial quantities of bitumen were produced (see O'Rourke et al., 1999, for

198   review). Flue gas was also injected at a later stage (Yee and Stroich, 2004) and the

199   project is now in a commercial stage. Separate vertical wells were drilled to monitor

200   temperature and deformations. About 5 cm of heave was recorded in the centre of the

201   deforming area from September 1993 to in April 1994, as shown in Figure 4. As the

202   project matured, the heave increased up to 30 cm in 2001.

203   Following the success of the UTF project, several commercial projects using SAGD

204   technology started, and are now producing in the Athabasca area. A complete set of

205   heave surveys is available for the MacKay River project of PetroCanada (Petro-Canada,

206   2008) and the Firebag project of Suncor (Suncor, 2008).

207   The MacKay River SAGD produces from the McMurry sand at a depth of about 100

208   m, at an operating pressure of 1.7 MPa and steam temperature of 205 °C. Deformations

209   were measured by repeated monitoring of 97 monuments (leveling) and supplemented

210   by an array of tiltmeters and microseismic monitoring. In December 2007, an additional

211   67 monuments were installed. The heave contours between the baseline surveys of

212   December 2002 and December 2007 are shown in Figure 5a. The overall heave pattern

213   follows the orientation of the injection/production well pairs running NE to SW. The

214   heave exceeds 30 cm in several areas and reaches a maximum of 37 cm over the field.

215   Heave along a profile oriented perpendicular to the well pairs is shown for three

216   different times in Figure 5b.

217   The Firebag project of Suncor also produces from the McMurry formation but it is in

218   an earlier stage of development. Heave surveys have been conducted yearly from 2004

219   to 2008 and the cumulative heave during this period has reached 15.3 cm, with the

220   incremental heave over the last year having a maximum of 4.9 cm. Coupled

221   geomechanical and thermal flow studies carried out by the authors on various Athabasca

222   sites confirm the range of uplift observed at the sites discussed above (i.e., 20-35 cm).

10

223 The main mechanisms contributing to heave include thermal expansion, decrease of the

224 effective stress, nonlinear decrease of stiffness associated with decrease of effective

225 stress and change in Poisson's ratio.

226 **3.2.   Injection for ASR**

227 *3.2.1. Santa Clara Valley and Santa Ana Basin, California*

228 The Santa Clara Valley is a structural trough running 110 km southeast of San

229 Francisco. The valley is bounded on the southwest by the Santa Cruz Mountains and the

230 San Andreas fault, and on the northeast by the Diablo Range and the Hayward fault.

231 The fresh-water-bearing sediments forming the groundwater reservoir within the valley

232 were mainly deposited during the Quaternary. They include semi-consolidated deposits

233 of the Pliocene and Pleistocene epochs, and unconsolidated alluvial and bay deposits of

234 the Pleistocene and Holocene epochs consisting of poorly sorted conglomerate,

235 sandstone, siltstone, and clay as much as 600 m thick. Coarse-grained deposits

236 predominate in the alluvial fans near the valley margins where the stream gradients are

237 steeper. The proportion of clay and silt layers increases toward the San Francisco Bay

238 (Poland, 1984).

239 From the early 1900s agriculture depended heavily on groundwater for irrigation. As

240 farming was progressively replaced by urban and industrial development in the 1940s,

241 the withdrawal continued to increase as the population grew. A decrease in rainfall

242 during the first half of the twentieth century along with an increase in the pumping rate

243 resulted in a significant drop of the artesian head, by as much as 80 m between 1912

244 and 1966. The well depth ranges from 90 to 360 m. Total annual groundwater

245 withdrawal approached 250 Mm^3 by 1960 (Ingebritsen and Jones, 1999). The

246 piezometric head decline caused as much as 4 m of land subsidence (Poland, 1984).

11

247   The Santa Clara Valley was the first area in the United States where organized

248   remedial actions were undertaken against groundwater overdraft with land subsidence

249   substantially halted by about 1969. Importation of surface water reduced the subsurface

250   pumping and allowed for an effective program of aquifer recharge leading to a recovery

251   of groundwater levels. Such a program began in the 1960s and continues presently.

252   Using InSAR Schmidt and Bürgmann (2003) showed the regional uplift of the ground

253   surface in the Santa Clara Valley occurred from 1992 to 1999 (Figure 6a). A maximum

254   upheaval of about 4 cm, reflecting the poroelastic response of the confined aquifer

255   system, has been measured northward. In the south-eastern part of the valley a seasonal

256   uplift signal is superimposed onto the long-term trend (Figure 6b). The long-term and

257   seasonal displacements result from head changes in the aquifer system in the elastic

258   range of stress. Observed water level fluctuations and borehole extensometer records

259   provide evidence that the vertical compressibility of the confined aquifer system in the

260   virgin stress range is from 20 to 100 larger than the average c_M in the elastic range

261   (Poland and Ireland, 1988).

262   InSAR investigations (Bawden et al., 2001) show that the 20×40 km Santa Ana

263   Basin in the metropolitan area of Los Angeles displays a seasonal fluctuation with a 5

264   cm uplift during the late fall through mid-spring (Figure 7) and 6 cm subsidence during

265   the late spring through mid-fall. Seasonal water table changes of the order of 30 m

266   indicate a close relationship between aquifer management and land deformation as

267   measured by InSAR. The aquifer is recharged all year round and is pumped during May

268   - September to meet the summer water demand. Approximately 78% of the water

269   pumped from the basin in 1996-1997 came from artificial recharge through surface

270   spreading basins located in the proximity of the Santa Ana River and Santiago Creek.

271   The produced water-bearing units span the depth interval between 50 and 600 m below

272   the ground surface (MWDSC, 2007).

12

273   *3.2.2. Las Vegas Valley, Nevada*

274   The Las Vegas Valley is located in a structurally controlled alluvial basin containing

275   up to 1500 m of unconsolidated sediments during the Pliocene through Holocene age.

276   Coarse-grained (sand and gravel) alluvial-fan deposits derived from the surrounding

277   mountain ranges form broad piedmonts around the periphery of the valley, while

278   predominantly fine-grained (silt and clay) compressible materials underlie the central

279   part of the valley. Intervening sequences of both coarse- and fine-textured sediments

280   give rise to a well-developed multi-aquifer system cut by several Quaternary faults

281   extending from the underlying bedrock to the ground surface. Most of the groundwater

282   in the aquifer system originates from the precipitation in the Spring Mountains to the

283   west.

284   Groundwater has greatly promoted the development of Las Vegas since the early

285   1900s when the first wells were drilled in the area. The Las Vegas metropolitan area

286   increased in population from 0.8 million in 1990 to more than 1.5 million in 2000.

287   Although natural springs historically provided water to this arid valley (the average

288   precipitation in a year is about 12-20 cm), groundwater pumping was drastically

289   increased to help meet the rising demand. Total pumpage reached a peak of more than

290   100 Mm^3/year in the late 1960s, remaining steadily above 70 Mm^3/year until the 1990s.

291   Groundwater is mainly pumped from the upper 600 m of unconsolidated sediments. The

292   long-term effects of pumping produced a regional decline of water levels of as much as

293   90 m by 1990 with more than 1.7 m of land subsidence measured by levelling surveys

294   through 2000 (Bell et al., 2002).

295   Since 1988 the Las Vegas Valley Water District (LVVWD) has maintained a

296   groundwater recharge program in to augment the local water supply during periods of

297   high demand. Water is recharged primarily in the coolest months using treated surface

298   water imported from the nearby Lake Mead on the Colorado River. Since the beginning

13

299 of the artificial recharge program, water levels have stabilized and recovered by as

300 much 30 m from 1990 to 2005 (LVVWD, 2005). Persistent Scatterer InSAR for the

301 periods 1995-2000 and 2003-2005 show a general reduction of the subsidence rate and a

302 broad area of uplift with velocities as much as 1 cm/year adjacent to the easternmost

303 margin of the main artificial recharge zone (Figure 8). Seasonal displacements of the

304 order of 1 cm are superimposed on the larger uplift trend, indicating that there are both

305 short- and long-term components in the elastic response of the system. The maximum

306 seasonal uplift occurs during January through March each year during the peak period

307 of artificial recharge (Amelung et al., 1999; Bell et al., 2008).

308 Based on the available subsidence/uplift measurements, the records of water level

309 changes, and the thickness of the compacting/expanding geologic units, the ratio r

310 between the inelastic (virgin loading) and elastic (unloading/reloading) compressibility

311 of the aquifer system has been estimated to be in the interval of 3 to 20 (Hoffmann et

312 al., 2001; Bell et al., 2008).

313 **3.3.   Injection for gas storage**

314 *3.3.1. Krechba field, Algeria*

315 The Krechba field is a gas reservoir located in the Algerian Sahara desert at a burial

316 depth of about 2000 m. The 20-m thick producing layer lies on a north-northwest

317 trending anticline and mainly consists of quartzose fine-grained sandstone of Early

318 Carboniferous period. The overburden comprises of a sequence of alternating

319 mudstones and sandstones. The horizontal stress field in the basin is highly anisotropic

320 with faults on the flanks of the anticline trending north-northwest. The gas produced

321 from the Krechba field contains a high mole fraction of CO_2 which must be separated

322 and disposed of for both economic and environmental reasons. The CO_2 is re-injected

323 into the reservoir through three nearby wells located at about 8 km northeast of the

14

324   cluster of the production wells. At the reservoir pressure the CO_2 behaves as a

325   supercritical fluid with a density of about 0.85 kg/dm^3. The well-head injection pressure

326   varies during the operations with an average value of 15 MPa and peak values achieving

327   18 MPa.

328   As part of a CO_2 sequestration research project, the PSInSAR technique (Ferretti et

329   al., 2001; Colesanti et al., 2003) has been used to monitor the injection effects on the

330   ground surface (Vasco et al., 2010). The study is based on satellite radar images

331   obtained from July 12, 2003 to March 19, 2007. With this approach, stable scatterers are

332   identified using a statistically based analysis of the phase and amplitude characteristics

333   of the energy reflected by the earth surface. A subset of such scatterers is denoted as

334   permanent and used to estimate the atmospheric and orbital errors. In the Krechba field

335   case the quality of the data is particularly good because the rock outcrops in the desert

336   area are stable reflectors. The mean vertical ground velocity for the investigated 2003-

337   2007 time interval as provided by the PSInSAR data analysis is shown in Figure 9. The

338   areas shown in blue are increasing in elevation by more than 5 mm/year and are clearly

339   correlated with the location of the three injection wells. The cumulative upheaval

340   measured above the Krechba field amounts to about 2 cm with a rather uniform areal

341   distribution.

342   *3.3.2. Lombardia field, Italy*

343   To cope with the energy demand in the cold season, gas and oil companies dispose of

344   methane in exhausted reservoirs during summer and extract it during winter. In Italy

345   Stogit S.p.A. manages a number of depleted gas fields for storage purposes. The

346   Lombardia field, located in the Po river plain, Northern Italy, is one such reservoir,

347   consisting of three mineralized layers (named A, B and C) made of turbiditic sediments

348   deposited during the late Pliocene epoch with about 30-m thick shale caprocks. Layer C,

15

349　about 100-m thick and 1200-m deep, is the main pool containing about 93% of the

350　overall gas originally in place. About 2,700 MSm^3 were produced from pool C between

351　1981 and 1986, and since 1986 pool C has been used for storage purposes. The largest

352　pore pressure drawdown achieved in 1986 was about 3 MPa. In the following years

353　water ingression from the surrounding aquifer led to a partial recovery of about 2 MPa.

354　Currently, the average operative pore pressure is about 1 MPa below the original value,

355　with a difference of 2.5 MPa between the maximum at the end of the storage phase and

356　the minimum at the end of withdrawal. The maximum pore pressure in the reservoir

357　exceeds the original in situ value by about 3% (IGU, 2003).

358　　An integrated monitoring system has been implemented above the Lombardia field to

359　monitor the land movements induced by the cyclic injection-extraction activity operated

360　in the reservoir. From 2003 to 2007 traditional high-precision levelling surveys were

361　carried out yearly along with a much more frequent PSInSAR analysis. The levelling

362　surveys reveal that the region above the field exhibits a slight upheaval trend with a

363　positive vertical ground velocity of about 1 mm/year. The PSInSAR data do show

364　cyclic ups and downs phased with the pressure variation within the reservoir. An

365　example of the vertical displacements vs. time for a few pixels from the PSInSAR

366　analysis located above the field is given in Figure 10, with the magnitude of the

367　occurrence gradually dissipating on the observation points farther from the reservoir.

368　Apart from the general upheaval trend, that is most likely of tectonic origin, land motion

369　appears to be elastic with an average difference between the peak values of about 1 cm.

370　A spatial kriging interpolation of the satellite images was used to map the areal

371　distribution of the vertical displacements above the reservoir. As an example, Figure 11

372　shows maps over the periods November 2005 – April 2006 (a) and April 2006 –

373　November 2006 (b). In the former time interval gas is withdrawn and land subsides, and

374　in the latter gas is injected and the land rises by about the same magnitude. Moving

16

375 farther from the reservoir boundary the vertical displacements quickly vanish and

376 appear to be un-influenced by gas storage.

377 A modeling study by Castelletto et al. (2010) and Teatini et al. (2010) shows that the

378 PS records are successfully matched with a finite element model using a loading

379 unloading-reloading compressibility ratio of 4.

380 **3.4. Injection for land subsidence mitigation**

381 *3.4.1. Wilmington, Long Beach, California*

382 The Wilmington oil field is a broad asymmetrical anticline extending lengthwise

383 approximately 18 km in a SE-NW direction and about 5 km in the SW-NE direction

384 below Long Beach, in the southwestern part of the Los Angeles basin, California. The

385 reservoir is made of seven overlying oil-bearing formations of the Pliocene and

386 Miocene epoch spanning the depth range 600-2000 m below m.s.l. The pools are

387 divided into six structural blocks by five major faults that restrict the fluid flow between

388 the blocks. The sediments predominantly comprise rather loose and unconsolidated

389 sands and siltstones, with intervening shale layers (Mayuga and Allen, 1970).

390 Because of limited waterdrive activity, the pressure decline in the oil reservoir was

391 relatively fast. By the mid-1960s about 9 MPa. of drawdown at 900 m depth, and nearly

392 9 m of land subsidence had occurred since the onset of production (Allen and Mayuga,

393 1970). The subsidence above the field was clearly recognized in 1941 when the U.S.

394 Coast and Geodetic Survey surveyed the levelling lines between San Pedro and Long

395 Beach, which had been previously monitored in 1933-1934. Subsequent measurements

396 showed increasing subsidence up to the maximum 9 m value experienced in 1965

397 (Colazas and Olson, 1983). Results from precision casing collar surveys, i.e. the

398 periodic monitoring of the shortening (or lengthening) of well casing joints due to the

17

399   compaction (or expansion) of the oil-bearing formations (Law, 1950), provided

400   evidence that compaction occurred over the 650-1100 m depth interval.

401   In order to mitigate land settlement a massive water injection program was

402   implemented in the late 1950s. Approximately 175,000 m^3/day of water were injected

403   into the field during the 1960s (Mayuga and Allen, 1970), declining to 90,000 m^3/day

404   by the mid-1990s (Otott Jr and Clark, 1996). Both seawater withdrawn from shallow

405   beds directly connected with the ocean and formation water produced along with the oil

406   were used for injection. Subsidence stopped over a large portion of the field with the

407   subsiding area reduced from 50 km^2 to 8 km^2. The settlement rate at the historical centre

408   of the subsidence bowl was reduced from a maximum of 71 cm/year in 1951 to zero in

409   1968, and in certain areas a surface rebound up to 33 cm was observed (Figure 12a). In

410   the newest portions of the Wilmington field waterflooding and oil production began

411   almost simultaneously. No significant subsidence occurred in those areas with over-

412   injection generating a 20 cm increase of the original ground elevation (Figure 12b)

413   (Colazas and Olson, 1983).

414   In-situ measurements by casing joints (Allen and Mayuga, 1970), lab tests at high

415   confining pressures (Vesiĉ and Clough, 1968) and numerical modelling (Kosloff et al.,

416   1980a, 1980b) suggest that the Wilmington sandy formations under unloading/reloading

417   are from 2 to 8 times stiffer than for virgin loading conditions.

418   *3.4.2. Tokyo and Osaka, Japan*

419   Over the 1950s-1960s a significant lowering of the groundwater level occurred in all

420   the major cities of Japan because of an uncontrolled overdraft of the shallow multi-

421   aquifer systems. For example, the resulting land settlement in Tokyo was reported to be

422   about 4.5 m relative to the ground elevation at the early 1920s (Yamamoto, 1995) with a

423   number of serious related social problems. Full scale development of the aquifer system

18

424 in Tokyo started in 1914. After that time, the number of deep wells increased very

425 quickly. The hydraulic head kept on falling year after year due to pumping from the

426 upper 300 m thick multi-aquifer, and after a temporary recovery during World War II, it

427 achieved its lowest value of about -70 m below the mean sea level of the Tokyo Bay

428 (Yamamoto, 1984).

429 To mitigate the anthropogenic settlement new regulations were established from the

430 early 1970s throughout Japan to control of the groundwater use. As a major

431 consequence groundwater level has increased over the last decades in all the major

432 Japanese cities, including Tokyo and Osaka, and this has been accompanied by a

433 general ground upheaval. This has been carefully monitored by local administrations in

434 order to prevent possible deformations of the underground structures. As an example,

435 Figure 13 shows the piezometric increase and the associated vertical uplift for the city

436 of Tokyo. Inspection of Figure 13a reveals the close relationship between aquifer

437 recovery occurring after the implementation of the 1970 regulations and land upheaval,

438 which amounts to about 20 cm. The areal distribution of the Tokyo uplift from 1991 to

439 2005 is shown in Figure 13b, with several zones experiencing an uplift of more than 5

440 cm and a slightly irregular pattern. Similar results are found for the city of Osaka where

441 several urban areas experienced uplift of about 3 cm in 5 years (Sreng et al., 2009).

442 *3.4.3. Taipei, Northern Taiwan*

443 Taipei City is the political and economical centre of Taiwan with a dense population

444 of about 3 million inhabitants plus several million people in the surrounding suburban

445 areas. Like many other big cities in the world, early development of the city was

446 enhanced by the development of the groundwater resources. The city centre lies on 300-

447 m thick late-Quaternary fluvial deposits laid down over deformed Miocene bedrock

448 starting from about 400,000 years ago.

19

449　　　　Groundwater pumping mainly occurred from 1955 to 1970 from a confined aquifer

450　　　lying between 50 and 140 m depth below the ground surface. Piezometric head has

451　　　decreased by more than 40 m with the lowest value reached in 1975. The massive

452　　　pumping was accompanied by large land settlements amounting to as much as 2.2 m in

453　　　the city centre (Wu, 1977). In order to mitigate the subsidence and prevent any possible

454　　　associated damages, the government stopped the use of groundwater in the Taipei Basin

455　　　during the early 1970s. The settlement rate has significantly decreased as the hydraulic

456　　　head gradually recovered and stabilized after approximately the late 1990s. The

457　　　establishment of a fine network of levelling benchmarks has allowed for accurate

458　　　monitoring and control of the ground movements during the recovery. The behaviour of

459　　　the post-pumping ground elevation is characterized by a relatively long period of

460　　　declining subsidence followed by a period of uplift from 1989 to 2003. Most surface

461　　　rebound was observed in the central to eastern portion of the basin, roughly

462　　　corresponding to the area of maximum subsidence. From 1989 to 2003 most of the

463　　　Taipei Basin, except for its westernmost margin, experienced a rather homogeneous

464　　　uplift of 7 to 10 cm with a maximum of 17 cm (Figure 14a). The largest rate, more than

465　　　1 cm/year, was measured between 1989 and 1994 (Figure 14b). The observed elastic

466　　　rebound was used to quantify a ratio of about 10 between the aquifer-system

467　　　compressibility under virgin loading and unloading/reloading conditions (Chen et al.,

468　　　2007).

469　　*3.4.4. Chioggia Mare, Northern Adriatic, Italy*

470　　　ENI-E&P, the Italian national oil company, has recently advanced a plan for the

471　　　development of a number of gas fields (about 15) located in the Northern Adriatic. The

472　　　largest field, named Chioggia Mare, is the closest to the coastline (the westernmost

473　　　margin of the field is 12 km from the city of Chioggia, south of Venice). Gas production

20

474   from Chioggia Mare raises some concerns about the risk of contributing to

475   anthropogenic settlement of Chioggia and the surrounding lagoon, including Venice. To

476   offset this environmental hazard ENI-E&P designed a project of land subsidence

477   mitigation using two deep seawater injection wells located halfway between the field

478   and the coastline. The Italian Ministry of Environment gave the University of Padova,

479   Department of Mathematical Models and Methods for the Scientific Applications

480   (DMMMSA), the task of checking the environmental sustainability of the ENI-E&P

481   mitigation programme, with the aid of ad hoc numerical models able to reliably predict

482   the expected land subsidence in the presence of the injection wells. The Chioggia Mare

483   gas field is seated at a 1100-1400 m depth and consists of four pools. The upper pools

484   (C and C2) are formed by a structural trap and the lower ones (E and Ea) pinch out

485   against a thick clayey formation (called Santerno), which represents a natural hydraulic

486   barrier. The estimated total gas withdrawn from Chioggia Mare over its 12-year

487   production life will be about 5,000 MSm^3. Pools C and C2 are surrounded by a strong

488   lateral and bottom waterdrive. The lateral aquifer partially encompassing pools E and

489   Ea is much weaker. More detailed information about the geology and the properties of

490   Chioggia Mare are provided in Teatini et al. (2000).

491   Injection of seawater is planned to take place in pool C lateral aquifer at a rate of

492   5,000 m^3/day for 25 years after the inception of gas production. The injected water will

493   be properly filtered to remove particles larger than 5-10 μm that could cause a reduction

494   of the aquifer permeability. It will be also chemically treated for compatibility with the

495   in situ water to avoid the activation of corrosion of the well intakes. Figures 15a and

496   15b show the simulated fluid pore pressure variation in pool C and the associated

497   waterdrive predicted at the end of the field production life without and with the injection

498   of water. It can be noted that the depressurization caused by gas pumping does not

499   propagate coastward because of the barrier effect exerted by the injection wells. Note

21

500   also the overpressure experienced by the waterdrive in the vicinity of the injection

501   boreholes. The simulated influence of injection on vertical ground displacement is

502   shown in Figures 15c and 15d. In the present case, water injection helps mitigate the

503   expected land subsidence and does not necessarily induce an appreciable anthropogenic

504   heave. Figure 16 shows the simulated vertical ground displacement in Chioggia without

505   and with the injection wells for the various plausible combinations of hydro-geo-

506   mechanical parameters investigated by Gambolati et al. (1998) in their report to the

507   Ministry. As an example, in the most favourable scenario using geomechanical

508   properties derived from lab tests, the predicted land uplift occurs 13 years after the

509   cessation of gas withdrawal and is on the order of 6 mm.

510   *3.4.5. Ravenna, Adriatic coastline, Italy*

511   The Ravenna Adriatic coastline is underlain by a major gas field, named Angela-

512   Angelina (Figure 17a), that extends down to 2900-4000 m depth and consists of a very

513   large number of gas pools (about 300) separated by intervening clayey layers and

514   crossed by a number of geological faults. Initially, the gas reserve was estimated to be

515   22,000 MSm^3 of which about 12,000 were produced as of January 2002 and 10,000

516   more are planned to be pumped out over the following 25-30 years. In a few depleted

517   pools the maximum fluid pore pressure drawdown has amounted to as much as 35 MPa.

518   The land subsidence caused by gas production in the vicinity of Angela-Angelina has

519   received the attention of a number of studies (Teatini et al., 1998; Gambolati et al.,

520   1999; Schroot et al., 2005) and is a matter of concern regarding the stability of the

521   Ravenna coastland. To mitigate it, ENI-E&P has implemented an experimental project

522   called "Angela Pressure Maintenance" with the final objective to oppose the anticipated

523   coastland settlement through the injection of water in the aquifer connected to the

22

524 reservoir over the depth interval 3100-3700 m. The ENI-E&P injection project was

525 designed in 2001 and consists of three phases (Figure 17b):

526   1- re-injection of the formation water, i.e. the water extracted along with the gas

527   from Angela-Angelina and the nearby offshore fields Amelia, Antares and Porto

528   Corsini Mare. At the beginning of the operation in 2003, the injection rate was

529   150 m^3/day and soon increased to 300 m^3/day with the addition of the seawater

530   obtained with the aid of the Beach Management System (BMS) (Ciavola, 2005;

531   Piccini et al., 2006) and chemically treated for compatibility with the situ water;

532   2- increase of the injection rate using additional wells from the cluster Angela;

533   3- further increase of the injection rate using the dismissed production wells from

534   the Angela-Angelina platform.

535   The cumulative water injected from March 2003 to April 2007 is shown in Figure

536 17c (ENI, 2007). Despite the very modest quantity of water injected underground some

537 benefits in terms of a delayed propagation of the depressurization below the coastline

538 have been observed. No evidence is so far available of any significant mitigation of land

539 subsidence. However, the ENI-E&P pressure maintenance experiment is of great

540 practical interest, and especially so in view of the planned progressively increased rate

541 of injection. Future modelling predictions and field measurements will help reveal the

542 hopefully effective impact of the above programme.

543   By the use of recent geophysical logs and marker measurements from deep offshore

544 boreholes drilled in the vicinity of Angela-Angelina, Baù et al. (2002) estimate a ratio r

545 between loading and unloading-reloading c_M ranging from 3 to 2 over the depth interval

546 3000–4000 m. However, because of the large injection depth, the medium

547 compressibility in expansion is expected to be about one order of magnitude smaller

548 than that of the shallower Chioggia Mare field.

23

549 **3.5.   Injection for geomechanical characterization. Upper Palatinate, Bavaria,**

550 **Germany**

551   A water injection experiment intended to study deformation of the upper crust,

552 improve knowledge of coupled hydro-geomechanical processes and characterize the

553 affected subsurface porous medium was performed from June 2004 to April 2005 in the

554 Upper Palatinate, Eastern Bavaria, Germany (Kumpel et al., 2006). Water was injected

555 at a rate of about 290 m^3/day to a total of 84,000 m^3 through an open hole that was

556 3850-4000 m deep. Land deformation was monitored by high-resolution borehole

557 tiltmeters installed at 5 locations (Berg, Eiglasdrof, Stockau, Mittelberg and

558 Pullersreuth) at a variable 1.5-3.3 km distance from the injection well denoted as

559 Kontinentale Tiefbohrung der Bundesrepublik Deutschland (KTB) (Jahr et al., 2005,

560 2006). The pore pressure increase exceeded 10 MPa at KTB over the injection time and

561 induced a land deformation that was detected by the tiltmeter array. The measured tilts

562 were reproduced with the aid of a finite element model. The results (Jahr et al., 2008)

563 reveal a maximum anthropogenic uplift of approximately 3 mm above the injection

564 point which dissipates quickly as one moves far from it (Figure 18a). Figure 18b shows

565 the modelling reconstruction of the tiltmeter measurements around KTB.

566 **4.   DISCUSSION AND CONCLUSIONS**

567   A survey of sites worldwide where underground fluid (water, gas, steam) injection

568 has caused a measurable land uplift (or heave) has been performed. Fluid is injected for

569 a variety of purposes, from enhancing oil production to storing gas in depleted gas/oil

570 fields, recharging pumped aquifers, disposing of industrial liquid wastes and mitigating

571 anthropogenic land subsidence. Vertical land displacement is measured using traditional

572 levelling, tiltmeters, or, most recently and relatively inexpensively, with the aid of the

573 satellite interferometry. Land may rise as a consequence of the migration to ground

24

574 surface of the injected formation expansion. This is due primarily to the release of the

575 effective intergranular stress and secondarily to the shear dilation (or dilatancy) on

576 condition that the induced fluid pore overpressure is large enough so as the yield surface

577 (or friction line) is intersected by the Mohr-Coulomb circles. Thermal expansion may

578 also contribute significantly to the observed heave. Careful inspection of each single

579 occurrence reveals that:

580   1- the observed land uplift may vary from a few millimetres to tens of centimetres

581   over a time interval of some months to several years according to the specific

582   location;

583   2- the largest uplift depends on a number of factors, including the fluid pore

584   pressure increase, the depth, thickness and areal extent of the pressurized and

585   heated geological formation, and the hydro-geo-thermo-mechanical properties of

586   the porous medium involved in the process.

587 The uniformity of uplift at the ground surface is basically related to the location,

588 arrangement, and strength of the injection sources and the depth of the injection that, in

589 turn, depend on the purpose of the disposal. If the injected formation is deep enough,

590 the uplift may be expected to be rather uniform for a regular distribution of the injection

591 wells. Conversely, if the injection is irregularly distributed and the injected formation is

592 shallow, the anthropogenic uplift may result in irregular patterns.

593 The case studies described above provide a clear affirmative answer to the question: is it

594 physically possible to appreciably raise the ground surface by injecting fluids

595 underground? This concern has been advanced by a few geotechnical and hydrological

596 experts (see Ferronato et al., 2008), in relation to a possible anthropogenic land uplift as

597 an innovative defence from periodical flooding that affect high-value coastal areas that

598 are experiencing land settlement and/or seal level rise due to climate changes. Recent

599 modeling studies (Comerlati et al., 2003, 2004) suggest that injecting seawater into a

25

600   600- to 800-meter-deep brackish aquifer underlying Venice, Italy, might induce an

601   upheaval of this much loved city by 25–30 cm over 10 years. Such an uplift would be

602   enough to offset the most likely scenario of relative sea level rise expected in 2100

603   (Carbognin et al., 2009).

604   A second point enlightened by the present survey regards the ratio r of virgin to second

605   cycle elastic compressibility c_M. The available data are summarized in Figure19 and

606   show that, almost irrespectively of the site, r tends to increase for shallower depth. If at

607   very large depths the virgin c_M is only from two to three times the elastic c_M, in shallow

608   aquifer systems (~50-300 m) the former can be one order of magnitude larger than the

609   latter. The actual prediction of the expected medium expansion due to fluid injection,

610   and thus the related ground uplift, requires the knowledge of c_M in the unloading-

611   reloading cycle. On first approximation, it might be obtained from the more frequently

612   and easily known c_M in virgin loading and a r estimate based on the depth of the

613   injected formation. For sure, a more accurate evaluation requires a site-specific

614   investigation. This is why, concerning the project mentioned above of anthropogenic

615   Venice raising, a pilot ad hoc injection experiment has been recently advanced

616   (Castelletto et al., 2008).

621

26

621 **REFERENCES**

622 Allen, D.R., Mayuga, M.N., 1970. The mechanics of compaction and rebound,

623   Wilmington oil field, Long Beach, California, USA. In Tjson, L.J., (Ed.), Land

624   Subsidence, Proceedings of the Tokyo Symposium 1969. IAHS Publication no. 89,

625   pp. 410-422.

626 Amelung, F., Galloway, D.L., Bell, J.W., Zebker, H.A., Laczniak, R.J., 1999. Sensing

627   the ups and downs of Las Vegas: InSAR reveals structural control of land subsidence

628   and aquifer-system deformation. Geology 27, 483-486.

629 Baù, D., Ferronato, M., Gambolati, G., Teatini, P., 2002. Basin-scale compressibility of

630   the Northern Adriatic by the radioactive marker technique. Geotéchnique 52, 605-

631   616.

632 Bawden, G.W., Thatcher, W., Stein, R.S., Hudnut, K.W., Peltzer, G., 2001. Tectonic

633   contraction across Los Angeles after removal of groundwater pumping effects.

634   Nature 412, 812-815.

635 Bell, J.W., Amelung, F., Ramelli, A., Blewitt, G., 2002. Land subsidence in Las Vegas,

636   Nevada, 1935-2000: New geodetic data show evolution, revised spatial patterns, and

637   reduced rates. Environmental and Engineering Geoscience 8, 155-174.

638 Bell, J.W., Amelung, F., Ferretti, A., Bianchi, M., Novali, F., 2008. Permanent scatterer

639   InSAR reveals seasonal and long-term aquifer system response to groundwater

640   pumping and artificial recharge. Water Resources Research 44, doi:

641   10.1029/2007WR006152.

642 Carbognin, L., Teatini, P., Tomasin A., Tosi, L., 2009. Global change and relative sea

643   level rise at Venice: what impact in term of flooding. Climate Dynamics,

644   doi:10.1007/s00382-009-0617-5.

27

645   Castelletto, N., Ferronato, M., Gambolati, G., Putti, M., Teatini, P., 2008. Can Venice

646   be raised by pumping water underground? A pilot project to help decide. Water

647   Resources Research, 44, W01408, doi:10.1029/2007WR006177.

648   Castelletto, N., Ferronato, M., Gambolati, G., Janna, C., Teatini, P., Marzorati, D.,

649   Cairo, E., Colombo, D., Ferretti, A., Bagliani, A., Mantica, S., 2010. 3D

650   geomechanics in UGS projects. A comprehensive study in northern Italy. In: Proc.

651   44th U.S. Rock Mechanics Symposium. American Rock Mechanics Association, in

652   press.

653   Chen, C.T., Hu, J.T., Lu, C.Y., Lee, J.C., Chan, Y.C., 2007. Thirty-year land elevation

654   change from subsidence to uplift following the termination of groundwater pumping

655   and its geological implications in the Metropolitan Taipei Basin, Northern Taiwan.

656   Engineering Geology 95, 30-47.

657   Ciavola, P., 2005. The new Beach Management System at Lido Adriano, Ravenna,

658   Italy. Footprints - ShoreGro Newsletter 3, 5-6.

659   Colazas, X.C., Olson, L.J., 1983. Subsidence monitoring methods and beach mark

660   elevation response to water injection, Wilmington oil field, Long Beach, California.

661   In Donaldson, E.C., and van Domselaar, H., (Eds.), Proceedings of 1982 Forum on

662   Subsidence due to Fluid Withdrawals, U.S. Government Printing Office, pp. 121-

663   132.

664   Colesanti, C., Ferretti, A., Novali, F., Prati, C., Rocca, F., 2003. SAR monitoring of

665   progressive and seasonal round deformation using the Permanent Scatterers

666   technique. IEEE Transactions of Geoscience and Remote Sensing 41, 1685-1701.

667   Collins, P.M., 2007. Geomechanical effects on the SAGD process. SPE Reservoir

668   Evaluation & Engineering 10(4), 367-375.

669   Comerlati, A., Ferronato, M., Gambolati, G., Putti M., Teatini, P., 2003. Can CO_2 help

670   save Venice from the sea? EOS Transaction AGU, 84(49), 546-553.

28

671   Comerlati, A., Ferronato, M., Gambolati, G., Putti M., Teatini, P., 2004. Saving Venice

672   by seawater. Journal of Geophysical Research, 109(F3), doi: 10.1029/2004JF000119.

673   Coussy, O., 1995. Mechanics of Porous Continua. Wiley, New York (NY).

674   de Koning, J., de Pater, H., Walters, D., Maxwell, S., 2008. Geomechanics for

675   interpreting SAGD monitoring using micro-seismicity and surface tiltmeters. Paper

676   SPE/PS/CHOA 117688, Int. Thermal Operations and Heavy Oil Symp., Calgary,

677   Alberta, Canada, 20-23 Oct. 2008, 20pp.

678   Donaldson, E.C., 1964. Surface disposal of industrial wastes in the United States.

679   Technical Report, U.S. Bureau of Mones, Washington D.C..

680   Du, J., Brissenden, S.J., McGillivray, P., Bourne, S., Hofstra, P., Davis, E.J.,

681   Roadarmel, W.H., Wolhart, S.L., Marsic, S., Gusek, R., Wright, C.A., 2005.

682   Mapping reservoir volume changes during cyclic steam stimulation using tiltmeter-

683   based surface-deformation measurements. Paper SPE/PS-CIM/CHOA 97848

684   PS2005-384, 2005 Int. Thermal Operations and Heavy Oil Symposium, Calgary, 1-3

685   November, 2005, 12pp.

686   Dusseault, M.B., Rothenburg, L., 1988. Shear dilatancy and permeability enhancement

687   in oil sands. In: Proceedings of the 4th UNITAR Conference Heavy Crude and Tar

688   Sand, vol. 3, pp. 55–66.

689   ENI S.p.A., 2007. Progetto sperimentale Angelina Pressure Maintenace – Rapporto

690   trimestrale alla Provincia di Ravenna, Marzo 2007. ENI S.p.A. – Divisione E&P

691   Report, 12 pp. (in Italian)

692   Ferretti, A., Prati, C., Rocca, F., 2001. Permanent scatterers in SAR interferometry.

693   IEEE Transactions on Geoscience and Remote Sensing 39, 8-20.

694   Ferretti, A., Novali, F., Bürgmann, R., Hilley, G., Prati, C., 2004. InSAR Permanent

695   Scatterer analysis reveals ups and downs in San Francisco Bay area. EOS

696   Transactions of the American Geophysical Union 85, 317-324.

29

697   Ferronato, M., Gambolati, G., Teatini, P., 2003. Unloading-reloading uniaxial

698   compressibility of deep reservoirs by marker measurements. In S. Stiros and S.

699   Pytharouli (Eds.), Proceedings of 11th International Symposium on Deformation

700   Measurements. Geodesy and Geodetic Applications Laboratory, Patras University,

701   pp. 341-346.

702   Ferronato, M., Gambolati, G., Putti, M., Teatini, P., 2008. A pilot project using seawater

703   to uplift Venice anthropogenically. EOS Transaction AGU, 89(15), 152.

704   Galloway, D.L., Hudnut, K.W., Ingebritsen, S.E., Phillips, S.P., Peltzer, G., Rogez, F.,

705   Rosen, P.A., 1998. Detection of aquifer system compaction and land subsidence

706   using interferometric synthetic aperture radar, Antelope Valley, Mojave Desert,

707   California. Water Resources Research 34, 2573-2585.

708   Galloway, D.L., Hoffmann, J., 2007. The application of satellite differential SAR

709   interferometry-derived ground displacements in hydrogeology. Hydrogeology

710   Journal 15, 133-154.

711   Gambolati, G., Teatini, P., Tomasi, L., 1998. Convenzione tra il Ministero

712   dell'Ambiente e l'Università degli Studi di Padova per la realizzazione di un modello

713   matematico previsivo degli eventuali effetti di subsidenza connessi alla coltivazione

714   di giacimenti di idrocarburi in Alto Adriatico. Technical Report, DMMMSA,

715   University of Padova, 179 pp. (in Italian)

716   Gambolati, G., Teatini, P., Tomasi, L., Gonella, M., 1999. Coastline regression of the

717   Romagna Region, Italy, due to natural and anthropogenic land subsidence and sea

718   level rise. Water Resources Research 35, 163-184.

719   Gambolati, G., Teatini, P., Ferronato, M., 2005. Anthropogenic land subsidence. In

720   Anderson, M.G., (Ed.), The Encyclopedia of Hydrological Sciences. John Wiley &

721   Sons, London, pp. 2443-2460.

30

722   Hoffmann, J., Zebker, H.A., Galloway, D.L., Amelung, F., 2001. Seasonal subsidence

723   and rebound in Las Vegas Valley, Nevada, observed by synthetic aperture radar

724   interferometry. Water Resources Research 37, 1551–1566.

725   Hoffmann, J., Zebker, H.A., 2003. Prospecting or horizontal surface displacements in

726   Antelope Valley, California, using satellite radar interferometry. Journal of

727   Geophysical Research 108 (F1), doi:10.1029/2003JF000055.

728   Ingebritsen, S.E., Jones, D.R., 1999. Santa Clara Valley, California. In: Galloway, D.L.,

729   et al. (Eds.), Land Subsidence in the United States, USGS Circular 1182, pp. 15-22.

730   International Gas Union, 2003. Underground Gas Storage Data Bank,

731   http://www.igu.org/html/wgc2003/WGC_pdffiles/data/IGU/IGU-UGS-World-Data-

732   Bank.mdb

733   Jahr, T., Jentzsch, G., Letz, H., Sauter, M., 2005. Fluid injection and surface

734   deformation at the KTB location: modelling of expected tilt effects. Geofluids 5, 20-

735   27.

736   Jahr, T., Letz, H., Jentzsch, G., 2006. Monitoring fluid induced deformation of the

737   earth's crust: a large scale experiment at the KTB location, Germany. Journal of

738   Geodynamics 41, 190-197.

739   Jahr, T., Jentzsch, G., Gebauer, A., Lau, T., 2008. Deformation, seismicity, and fluids:

740   results of the 2004/2005 water injection experiment at the KTB, Germany. Journal of

741   Geophysical Research 113 (B11430), doi:10.1029/2008JB005610.

742   Kosloff D., Scott R.F., Scranton J., 1980a. Finite element simulation of Wilmington oil

743   field subsidence: I. Linear modelling. Tectonophysics 65, 339-368.

744   Kosloff D., Scott R.F., Scranton J., 1980b. Finite element simulation of Wilmington oil

745   field subsidence: II. Nonlinear modelling. Tectonophysics 70, 159-183.

746   Kumpel, H.J., Erzinger, J., Shapiro, S., 2006. Two massive hydraulic tests completed in

747   deep KTB borehole. Scientific Drilling Journal 3, 40-42.

31

748   Law., J., 1950. Interrelations between earth movements. Report to the Harbor

749   Commissioners, City of Long Beach, p. 94.

750   Las Vegas Valley Water District, 2005. 2005 Artificial recharge annual report. Las

751   Vegas Valley Water District Unpublished Report, 150 pp.

752   Mayuga, M.N., Allen, D.R., 1970. Subsidence in the Wilmington Oil Field, Long

753   Beach, California, USA. In Tjson, L.J., (Ed.), Land Subsidence, Proceedings of the

754   Tokyo Symposium 1969. IAHS Publication no. 88, pp. 66-79.

755   McGillivray, P.R., Brissenden, S., Bourne, S., Maron, K., Bakker, P., 2006. Making

756   sense of the geomechanical impact on the heavy-oil extraction process at Peace River

757   based on quantitalive analysis and modeling. Paper SPE 102876, 2006 SPE Annual

758   Tech. Conf., San Antonio, Texas, USA, 24-27 Sept. 2006, 5 pp.

759   Metropolitan Water District of Southern California, 2007. Groundwater Assessment

760   Study. Report Number 1308.

761   O'Rourke, J.C., Begley, A.G., Boyle, H.A., Yee, C.T., Chambers, J.I., Luhning, R.W.,

762   1997. UTF Project Status Update May 1997. Journal of Petroleum Technology 38(9),

763   44-54.

764   Otott Jr., G.E., Clarke, D.D., 1996. History of the Wilmington field - 1986-1996. In:

765   AAPG Pacific Section, Old Oil Fields and New Life: A Visit to the Giants of the Los

766   Angeles Basin, pp. 17–22.

767   Petro-Canada, 2008. MacKay River Performance Presentation Approval No. 8668.

768   Petro-Canada report to ERCB, accessible at:

769   http://www.ercb.ca/docs/products/osprogressreports/2008/2008AthabascaPetroCanad

770   aMacKayRiverSAGD8668.zip

771   Piccini, M.F., Gonella, M., Teatini, P., Gabbianelli, G., 2006. Modeling groundwater

772   response to beach dewatering at Ravenna shoreline. In A. Micallef et al. (Eds.),

773   Proceedings of 2nd International Conference on Management of Coastal Recreational

32

774   Resources – Beaches, Yachting and Coastal Ecotourism. Euro Mediterranean Centre

775   on Insular Coastal Dynamics Publisher, University of Malta, pp. 169-178.

776   Poland, J.F., Ireland R. L. (1988). Land subsidence in the Santa Clara valley, California,

777   as of 1982, mechanics of aquifer systems, U.S. Geol. Surv., Prof. Pap., 497-F, 61 pp.

778   Rintoul, W., 1981. The case of the disappearing land. In: Drilling Ahead: Tapping

779   California's Richest Oil Fields. Valley Publ., Santa Cruz (CA), pp. 116-137.

780   Schmidt, D.A., Bürgmann, R., 2003. Time dependent land uplift and subsidence in the

781   Santa Clara Valley, California, from a large InSAR data set. Journal of Geophysical

782   Research 108 (B9), doi:10.1029/2002JB002267.

783   Schroot, B.M, Fokker, P.A., Lutgert, J.E., van der Meer, B.G.H., Orlic, B., Scheffers,

784   B.C., 2005. Subsidence induced by gas production: an integrated approach. In:

785   Barends, F.B.J. et al. (Eds.), Land Subsidence-Special Volume (Proceedings of 7th

786   International Symposium on Land Subsidence). Millpress Science Publishers,

787   Rotterdam (The Netherlands), pp. 121-136.

788   Settari, A., Kry, P.R., Yeh, C.T., 1989. Coupling of fluid flow and soil behavior to

789   model injection into uncemented oil sands. Journal of Canadian Petroleum

790   Technology 28, 81-92.

791   Settari, A., Ito, Y., Fukushima, N., Vaziri, H., 1993. Geotechnical aspects of recovery

792   processes in oil sands. Canadian Geotechnical Journal 30, 22-33.

793   Sreng, S., Li, L., Sugiyama, H., Kusaka, T., Saitoh, M., 2009. Upheaval phenomenon in

794   clay ground induced by rising groundwater level. In H.I. Ling et al. (Eds.),

795   Poromechanics IV, to appear.

796   Stancliffe, R.P.W., van der Kooij, M.W.A.. 2001. The use of satellite-based radar

797   interferometry to monitor production activity at the Cold Lake heavy oil field,

798   Alberta, Canada. The American Association of Petroleum Geologists Bulletin 85(5),

799   781-793.

33

800 Suncor, 2008. 2008 ERCB Annual Review Suncor Firebag. Suncor Report to ERCB,

801   accessible at:

802   http://www.ercb.ca/docs/products/osprogressreports/2008/2008AthabascaSuncorFire

803   bagSAGD8870.pdf

804 Teatini, P., Gambolati, G., Tomasi, L., Putti, M., 1998. Simulation of land subsidence

805   due to gas production at Ravenna coastline. In G. Gambolati (Ed.), CENAS,

806   Coastline Evolution of the Upper Adriatic Sea due to Sea Level Rise and Natural and

807   Anthropogenic Land Subsidence. Kluwer Academic Publisher, Water Science and

808   Technology Library No. 28, pp. 133-150.

809 Teatini, P., Baù, D., Gambolati, G., 2000. Water-gas dynamics and coastal land

810   subsidence over Chioggia Mare field, Northern Adriatic sea. Hydrogeology Journal

811   8, 462-479.

812 Teatini, P., Gambolati, G., Castelletto, N., Ferronato, M., Janna, C., Marzorati, D.,

813   Cairo, E., Colombo, D., Ferretti, A., Bagliani, A., Bottazzi, F., Rocca, F., 2010.

814   Monitoring and modelling 3D ground movements induced by seasonal gas storage in

815   deep reservoirs. In: EISOLS 2010, Proceedings of the 8th Int. Symp. on Land

816   Subsidence. IAHR, in press.

817 United States Environmental Protection Agency, 2002. Technical program overview:

818   Underground injection control regulation. Tech. Rep. EPA 816-R-02-025, 81 pp.,

819   Washington, D. C.

820 Vasco, D. W., Rucci, A., Ferretti, A., Novali, F., Bissell, R. C., Ringrose, P. S.,

821   Mathieson, A. S., Wright, I. W., 2010. Satellite-based measurements of surface

822   deformation reveal fluid flow associated with the geological storage of carbon

823   dioxide. Geophysical Research Letters, 37, L03303, doi:10.1029/2009GL041544.

824 Vesiĉ, A.S., Clough, G.W., 1968. Behaviour of granular soils under high stresses.

825   ASCE, Soil Mechanics and Foundation Division, pp. 661-687.

34

826   Walters, D.A., 2007. Coupled geomechanical and reservoir simulation of the UTF

827   Phase B pilot project. Final Report to the Joint Industry Consortium, TAURUS

828   Reservoir Solutions Ltd., January 2007.

829   Wang, G., Kry, P.R., 1997. Surface heave due to fluid and steam injection. In:

830   Proceedings of 48th Annual Technical Meeting of the Petroleum Society, Calgary,

831   Alberta (CA), paper 97-10, 18 pp.

832   Watson, K.M., Bock, Y., Sandwell, D.T., 2002. Satellite interferometric observations of

833   displacements associated with seasonal groundwater in the Los Angeles basin.

834   Journal of Geophysical Research 107 (B4), doi: 10.1029/2001JB000470.

835   Wong, R.C.K., Lau, J., 2008. Surface heave induced by steam stimulation in oil sands

836   reservoirs. Journal of Canadian Petroleum Technology 47(1), 13-17.

837   Wu, C.M., Groundwater depletion and land subsidence in Taipei Basin. In Rodda, J.C.

838   (Ed.), Land Subsidence, Proceedings of 2nd International Symposium on Land

839   Subsidence. IAHS Publication No. 121, pp. 389-398.

840   Yamamoto, S., 1984. Case history no. 9.4: Tokyo, Japan. In Poland, J.F. (Ed.),

841   Guidebook to Studies of Land Subsidence Due to Ground-water Withdrawal. U.N.

842   Educational Science and Cultural Organ., Paris, pp. 175-184.

843   Yamamoto, S., 1995. Recent trend of land subsidence in Japan. In F.B.J. Barends et al.

844   (Eds.), Land Subsidence, Proceedings of 5th International Symposium on Land

845   Subsidence. IAHS Publication No. 234, pp. 487-492.

846   Yee, C.-T., Stroich, A., 2004. Flue gas injection into a mature SAGD steam chamber at

847   the Dover Project (Formerly UTF). Journal of Canadian Petroleum Technology

848   43(1), 54-61.

849

849 **FIGURE CAPTIONS**

850 **Figure 1.** Mohr-Coulomb circles. When the pore pressure p increases because of fluid

851 injection, the circles move leftward and may achieve the limiting yield surface or

852 friction line $\tau = c + \sigma_n \tan\phi$ where σ and τ are the normal and shear stress, respectively,

853 c is cohesion and ϕ the friction angle. τ_m and $\tau m*$ are the current largest and maximum

854 allowable shear stress, respectively, σ_1 and σ_3 the maximum and minimum principal

855 stress, respectively.

856 **Figure 2**. (a) Differential heave in 3 pads of the Cold Lake CSS during one steam

857 injection period (modifed from Wong and Kry, 1997). The upper figure is the total

858 heave at the beginning of the period, and the lower figure is the incremental heave

859 between the beginning and the end of the one month period. (b) Deformations over a

860 time period of 86 days (August 5, 1996 – November 1, 1996) measured by InSAR in

861 Cold Lake CSS project (adapted from Stancliffe and van der Kooij, 2001). Uplift is

862 positive.

863 **Figure 3**. Heave (a) over a one-year period and (b) from April 26, 2005 to June 5, 2005

864 calculated by tiltmeter data in the Shell Canada Peace River CSS project (modified from

865 Du et al., 2005).

866 **Figure 4**. Distribution of heave with depth from September 1993 to April 1994 at the

867 UTF BE2 extensometer site (adapted from Collins, 2007).

868 **Figure 5**. Heave (a) in the MacKay River SAGD project from December 2002 to

869 December 2007. The leveling monuments used to map the ground displacements are

870 shown. (b) Heave development in time along the cross section AB traced in (a)

871 (modified from Petro-Canada, 2008).

872 **Figure 6.** Vertical land displacement recorded by Differential InSAR in the Santa Clara

873 Valley, California. (a) Cumulative uplift measured from September 1992 to October

874 1999; (b) seasonal upheaval measured from August 1998 to March 1999. The bottom

36

875 insets shows the time series at two points illustrating the seasonal vs. long-term

876 deformation pattern partitioned by the Silver Creek (modified after Schmidt and

877 Bürgmann, 2003; Galloway and Hoffmann, 2007).

878 **Figure 7**. (a) Ground displacement in the Santa Ana Basin, California, detected by

879 Differential InSAR from July 1998 to January 1999. (b) Uplift behaviour along the A-

880 A' cross-section traced in (a) (modified after Bawden et al., 2001).

881 **Figure 8.** Velocity map for the northwest portion of Las Vegas Valley, Nevada,

882 obtained by Persistent Scatterer InSAR from ENVISAT data between April 2003 and

883 May 2005. The contour lines of the water-level change (m) recorded in the same

884 interval are shown. The inset on the right shows the time series of the vertical

885 displacement for the persistent scatterer indicated on the map (modified after Bell et al.,

886 2008).

887 **Figure 9.** Mean land vertical velocity above the Krechba field, Algeria, as detected by

888 the analysis of PSInSAR data in the period 2003-2007 (modified after Vasco et al.,

889 2010).

890 **Figure 10.** Vertical displacements (mm) vs. time for a few pixels monitored by InSAR

891 located above the Lombardia field, northern Italy.

892 **Figure 11.** Land vertical displacements above the Lombardia field between: (a)

893 November 2005 and April 2006; (b) April 2006 and November 2006. The maps are

894 obtained with a kriging interpolation of InSAR data. The reservoir outline is also

895 shown.

896 **Figure 12.** (a) Land uplift (inches) at Long Beach, California, from 1958 to1975 as a

897 result of elastic unloading caused by repressurization of the producing field blocks

898 (modified after Kosloff et al., 1980b). (b) Increase in elevation (feet) measured at a

899 leveling benchmark above a eastern block of the Wilmington field (modified after

900 Colazas and Olson, 1983).

37

901 **Figure 13.** Ground upheaval in Tokyo: (a) groundwater level and vertical displacement

902 over period 1962-2005; (b) cumulative upheaval distribution in the urban area over the

903 period 1991-2005 (modified after Sreng et al., 2009).

904 **Figure 14**. (a) Map of land uplift in the Taipei basin from 1989 and 2003 as obtained by

905 interpolation of the leveling records. (b) Land upheaval rate over the period 1989-1994

906 (modified after Chen et al., 2007).

907 **Figure 15.** Fluid pore pressure change (10^{-1} MPa, above) and anthropogenic land

908 subsidence (cm, below) at the end of the Chioggia Mare gas field production life as

909 predicted with the aid of numerical models: (a) and (c) without, (b) and (d) with the

910 seawater injection wells. Negative values denote pressure decline, positive values

911 pressure increase. The outline of the Chioggia Mare reservoir is also shown (modified

912 after Teatini et al., 2000).

913 **Figure 16.** Anthropogenic land subsidence and land heave in Chioggia as predicted

914 with the aid of numerical models without (solid lines) and with (dashed lines) seawater

915 injection wells for the various hydro-geo-mechanical scenarios addressed by Gambolati

916 et al. (1998).

917 **Figure 17.** (a) Location of the Angela-Angelina gas field along the Northern Adriatic

918 coastline, Italy. The trace of the reservoir is highlighted in red. (b) Representation of the

919 three-phase ENI-E&P injection programme "Angela Pressure Maintenance". (c)

920 Cumulative volume of water injected from March 2003 to April 2007 in the ENI-E&P

921 injection programme "Angela Pressure Maintenance".

922 **Figure 18.** Results from the finite element interpretation and reconstruction of the

923 tiltmeter measurements: (a) land uplift; (b) tilts at the land surface (modified after Jahr

924 et al., 2008).

925 Figure 19. Ratio *r* between virgin and second cycle elastic compressibility versus depth

926 as derived from the case studies addressed in the present paper (1: Santa Clara Valley,

38

927   California; 2: Las Vegas Valley, Nevada; 3: Lombardia field, Italy; 4: Wilmington,

928   California; 5: Taipei, Taiwan; and 6: Ravenna, Italy).

39

Figure 1

Figure 2

(a)

(b)
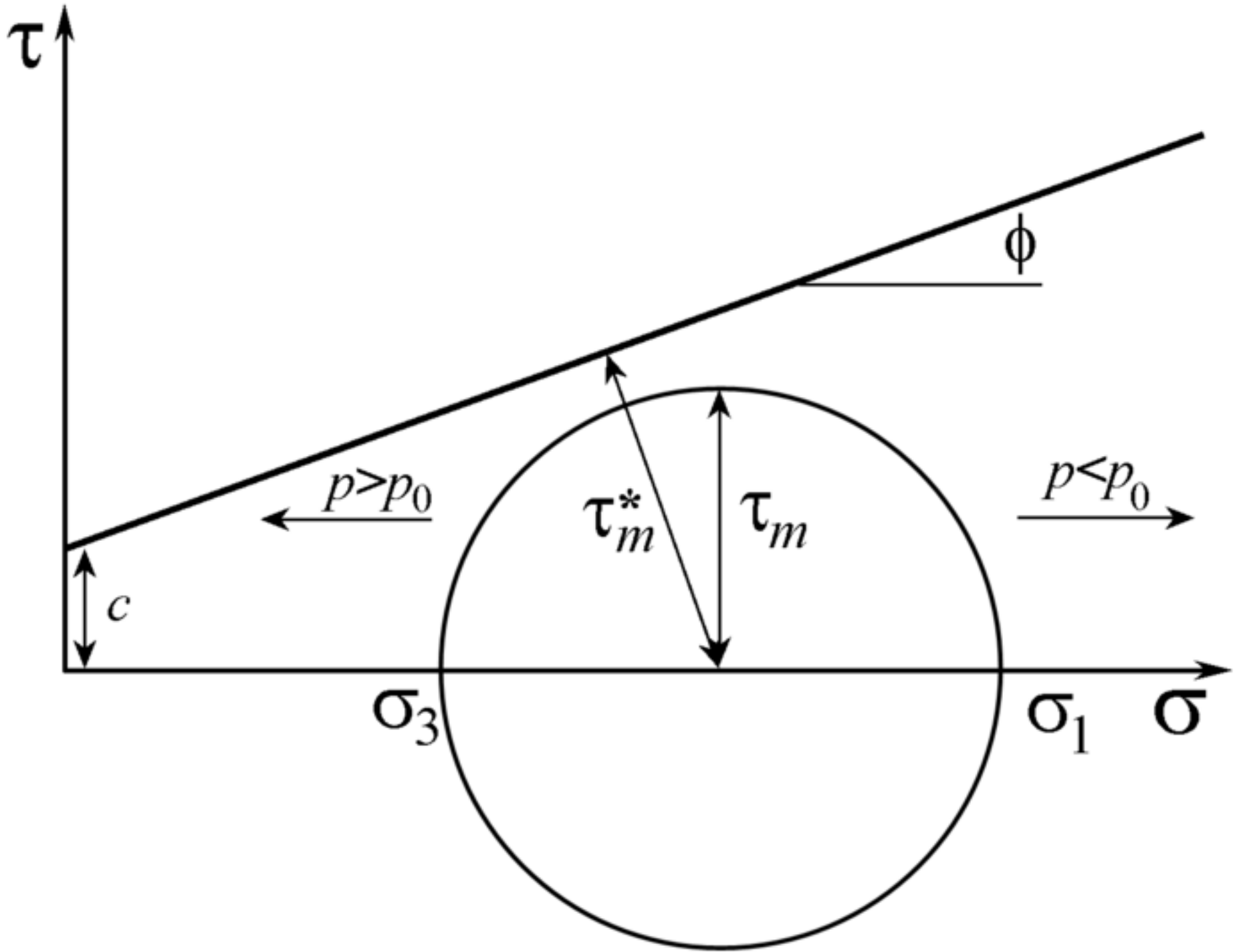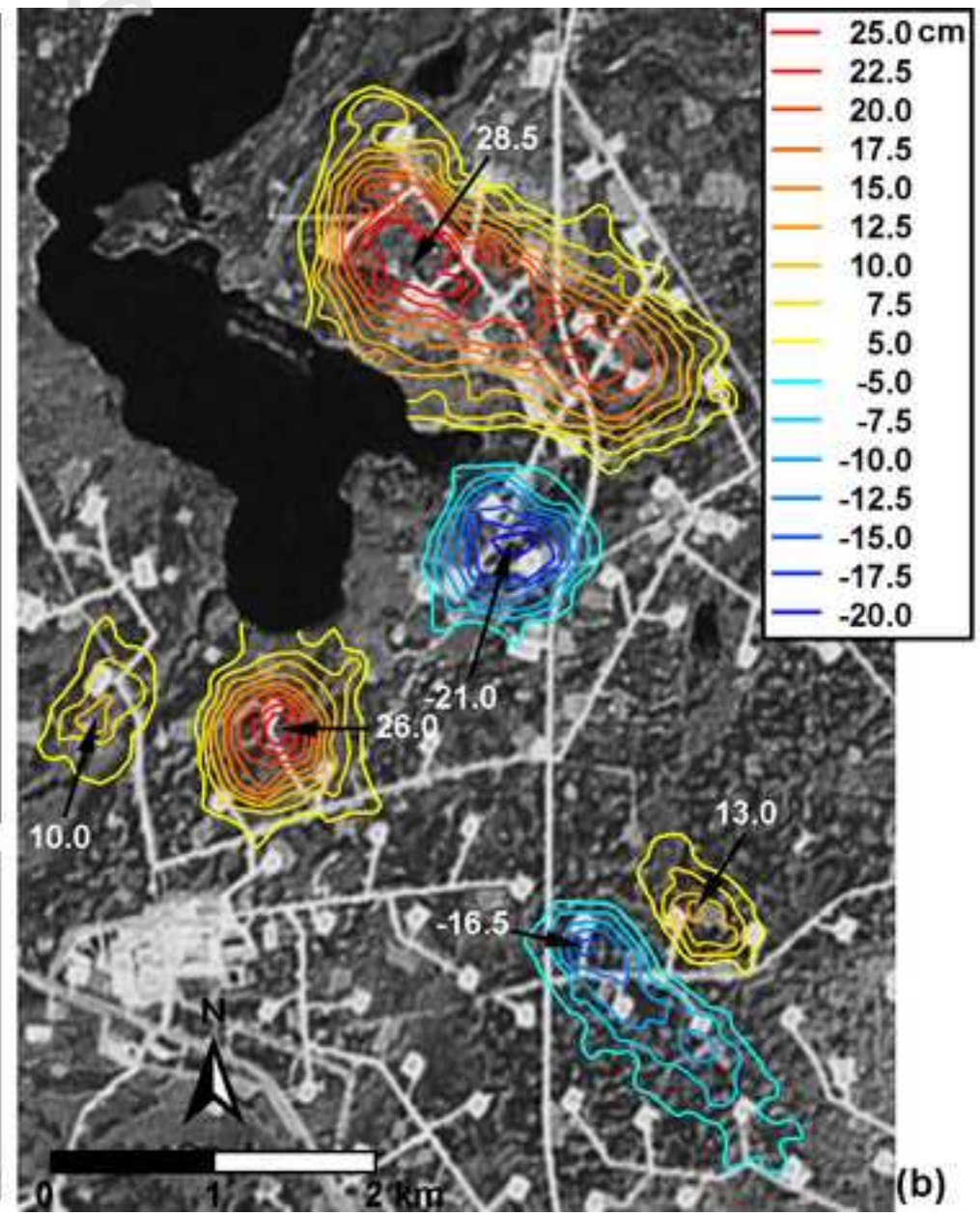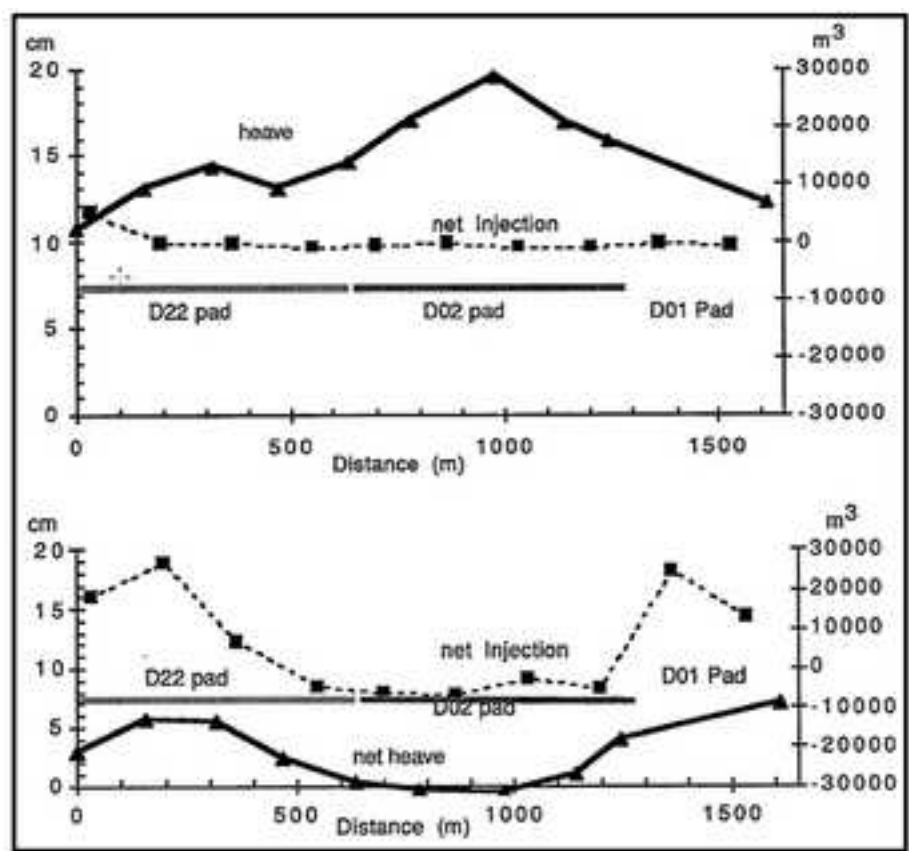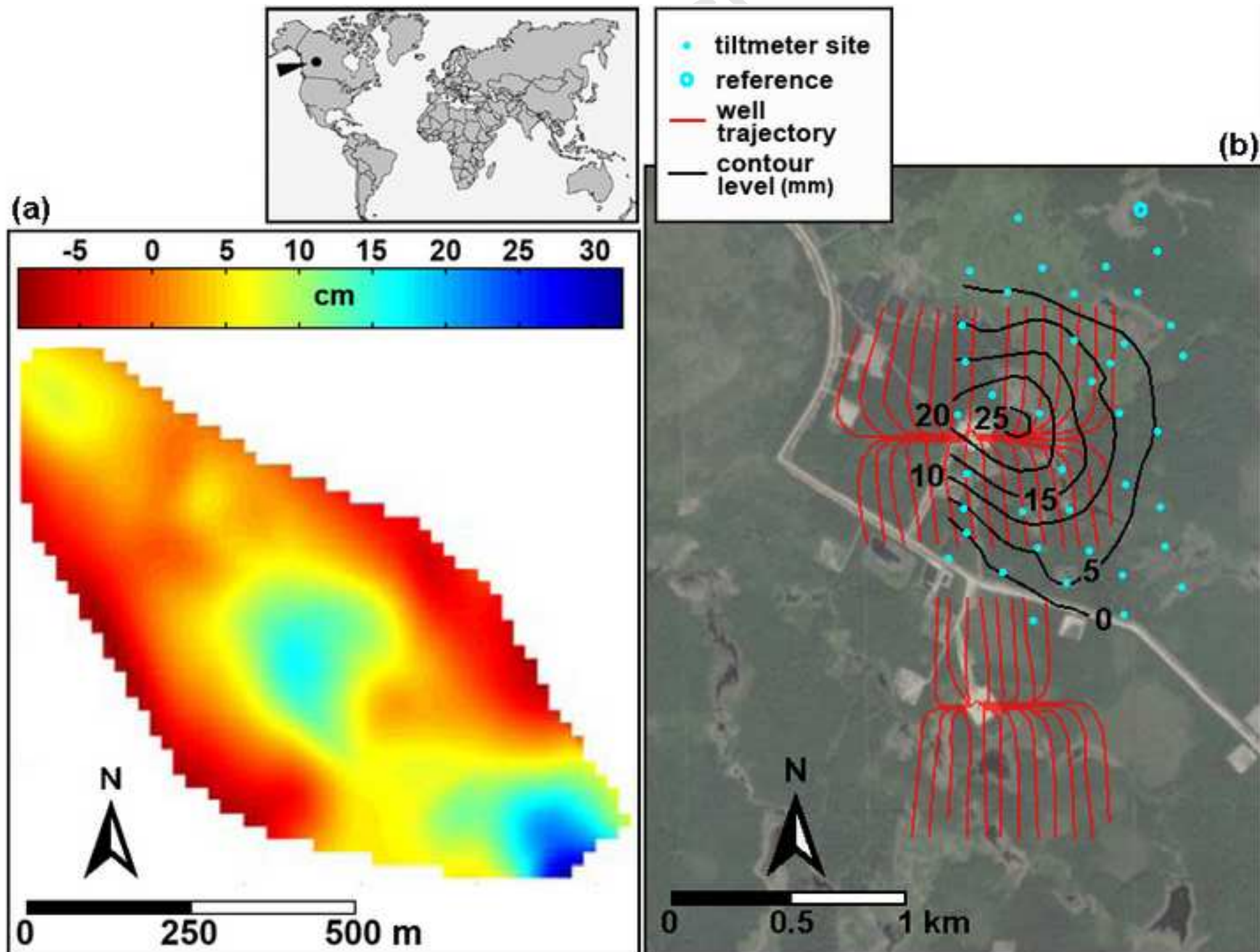
Figure 3

Figure 4

Figure 5

Figure 6

(a)

(b)
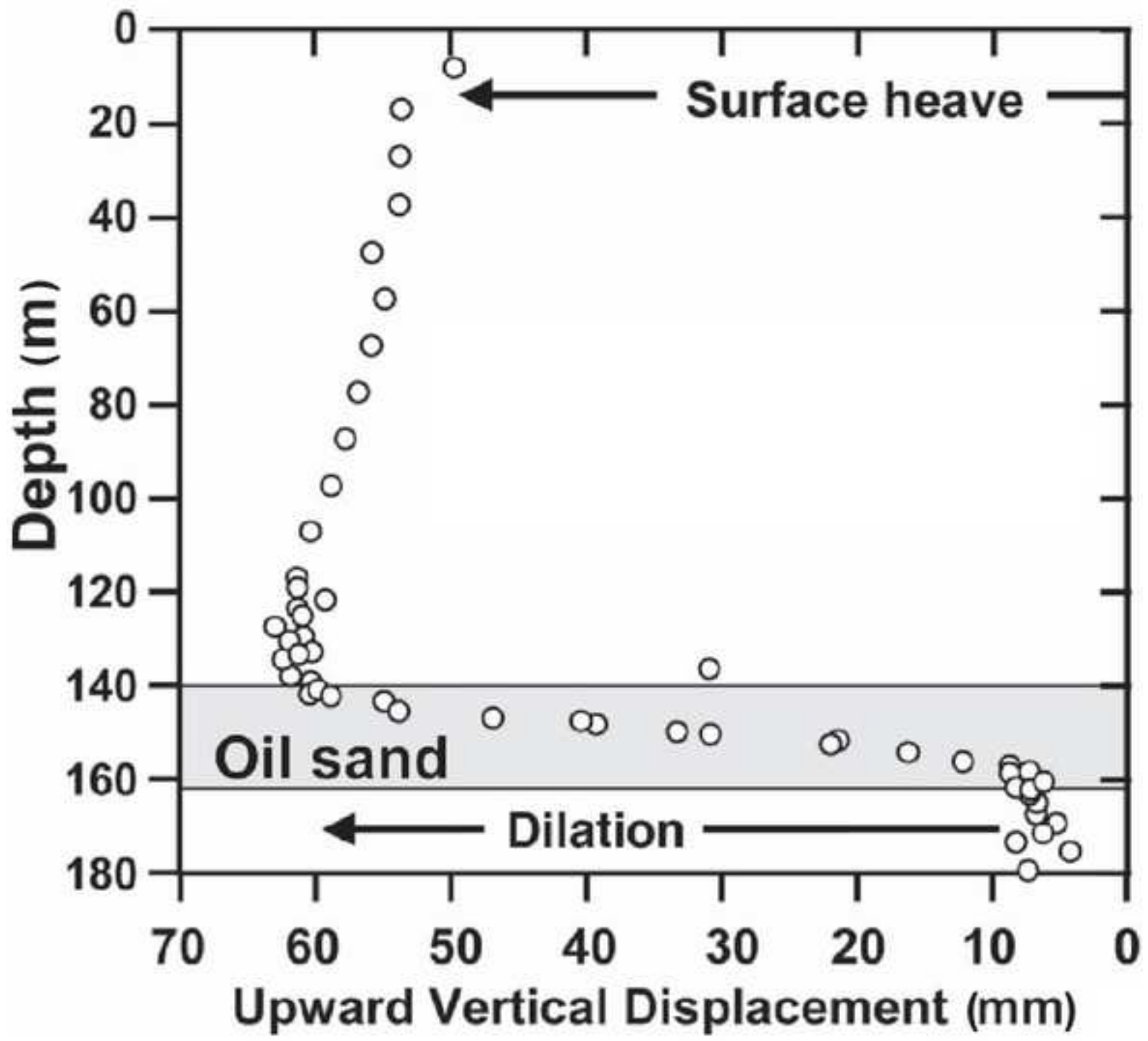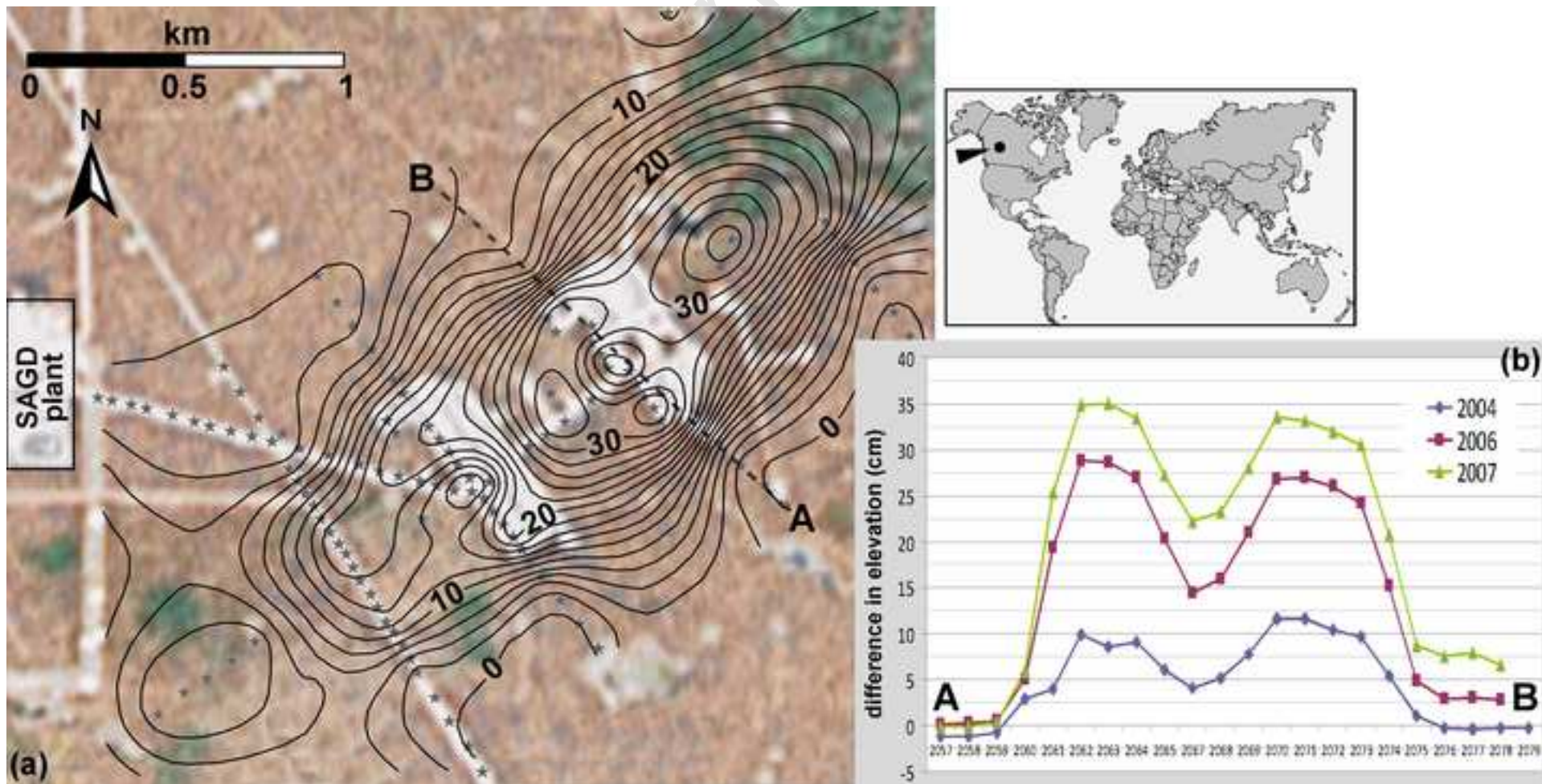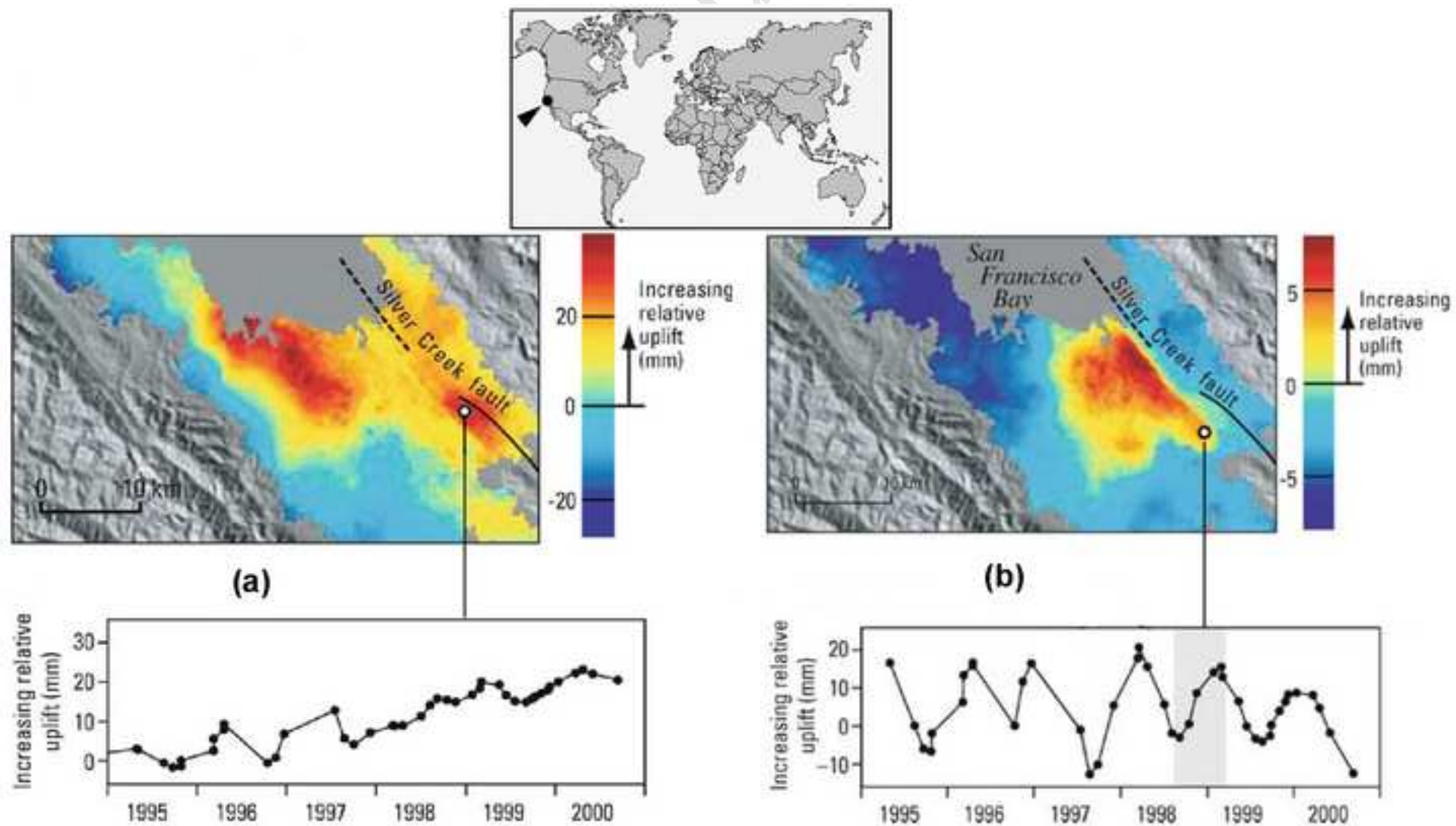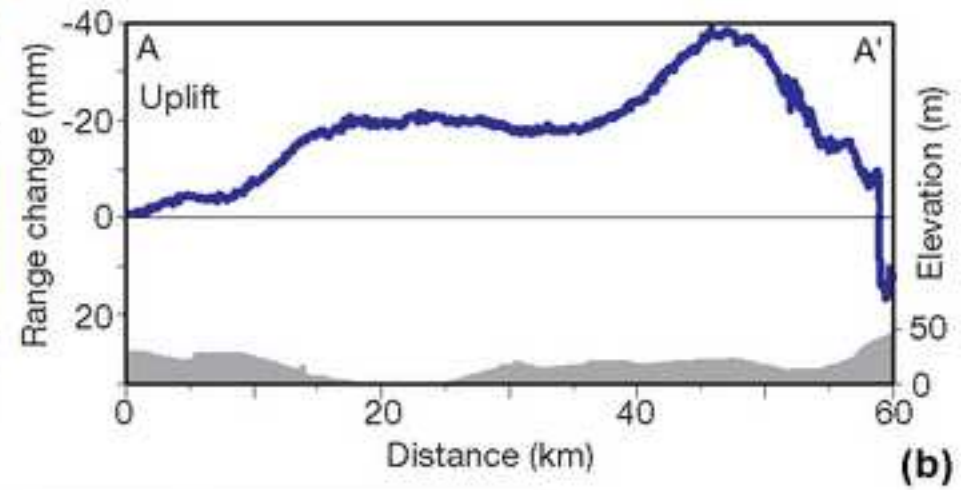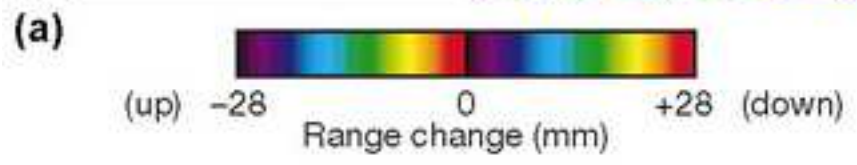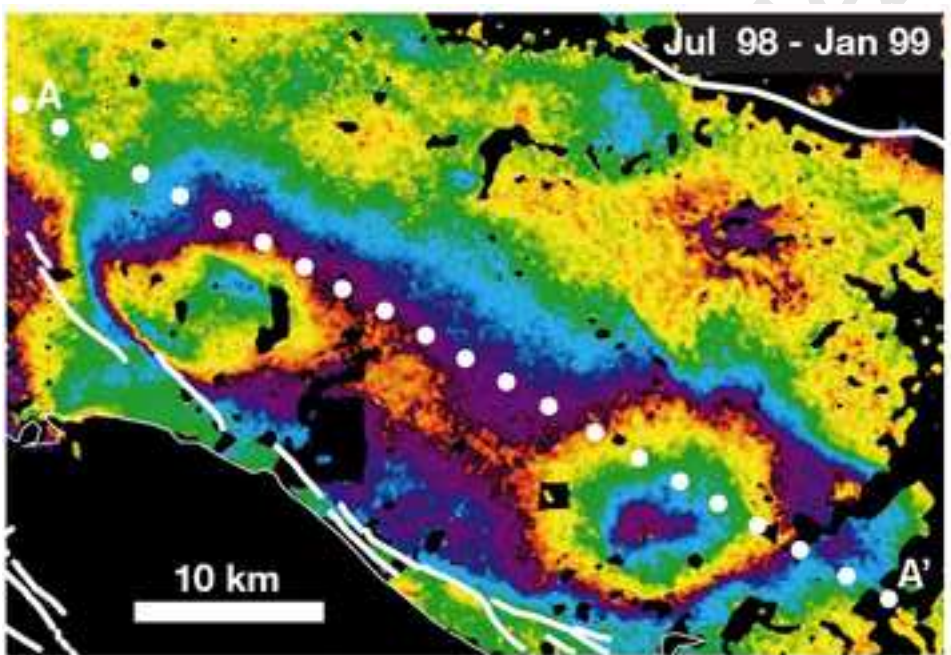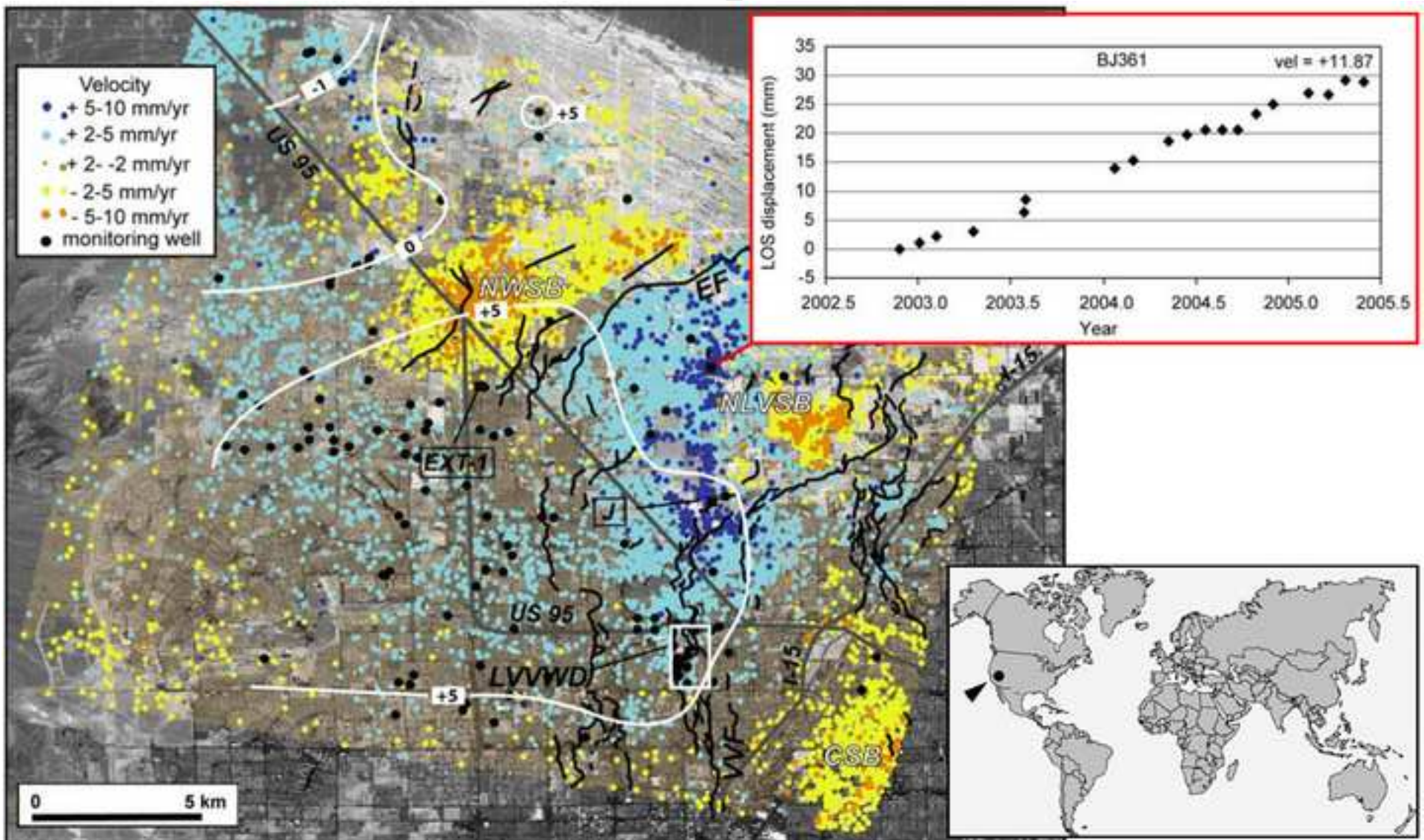
Figure 7

Figure 8

Figure 9

Figure 10

Figure 11

(a)

(b)

0   10   20 km
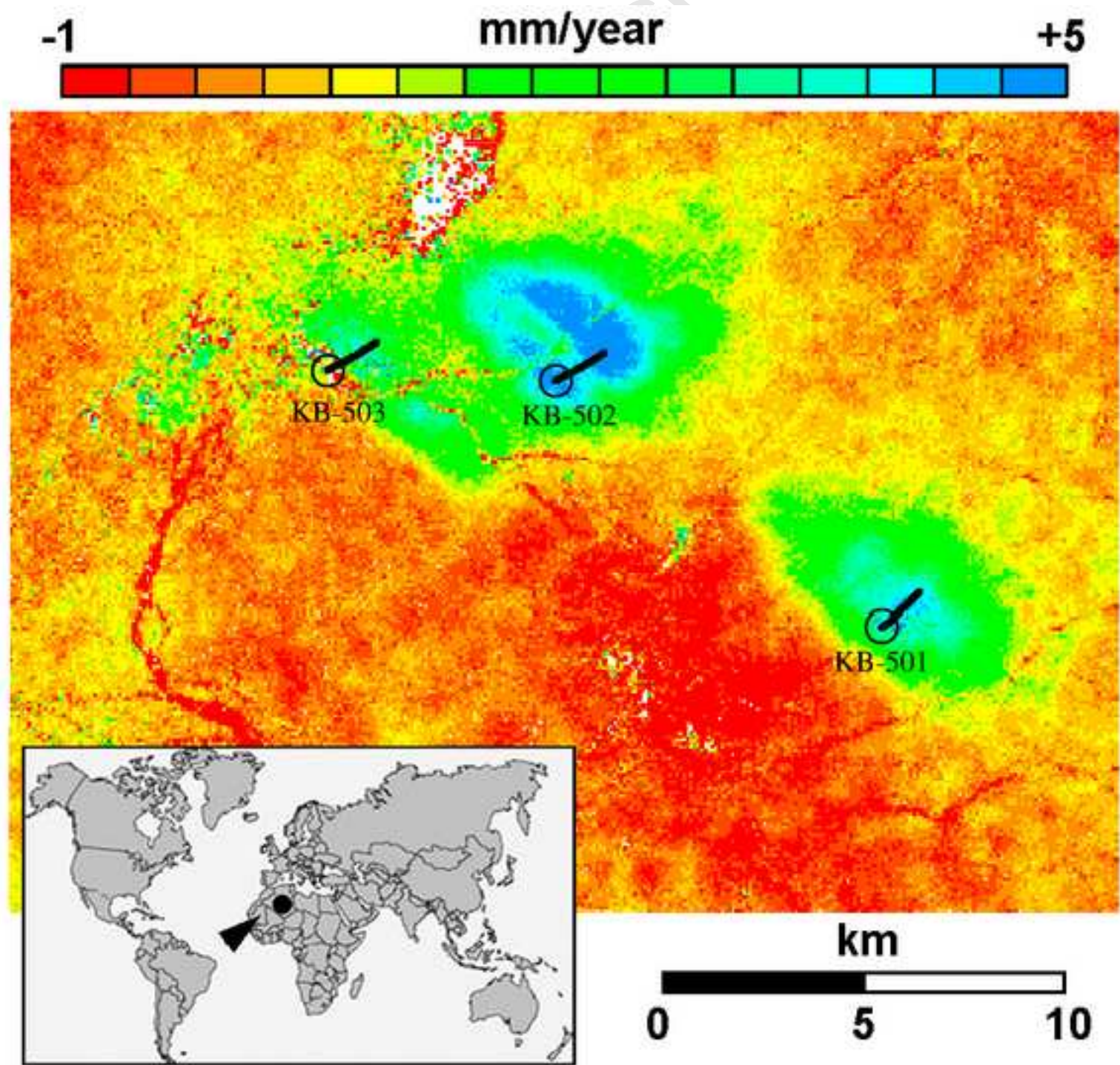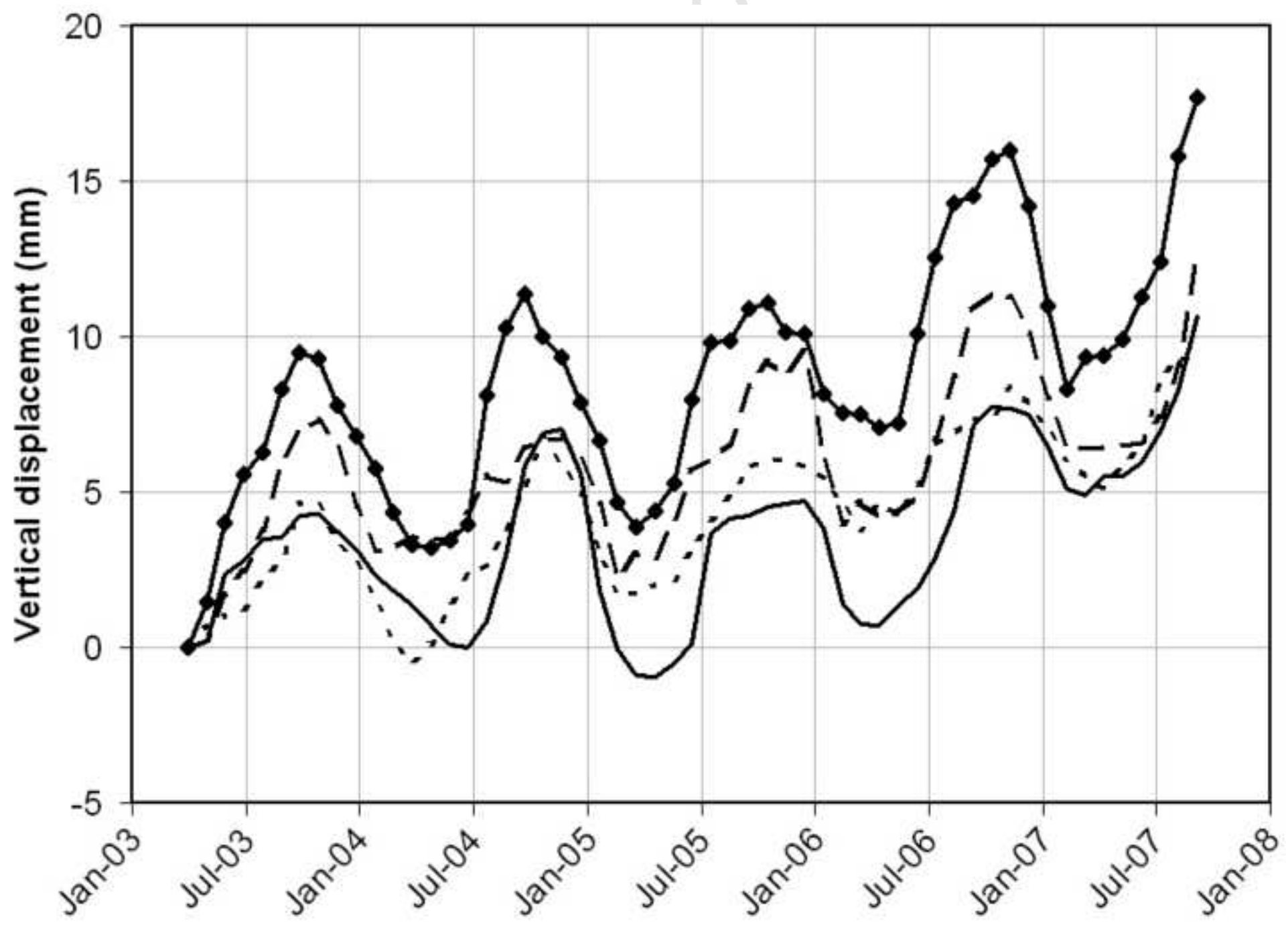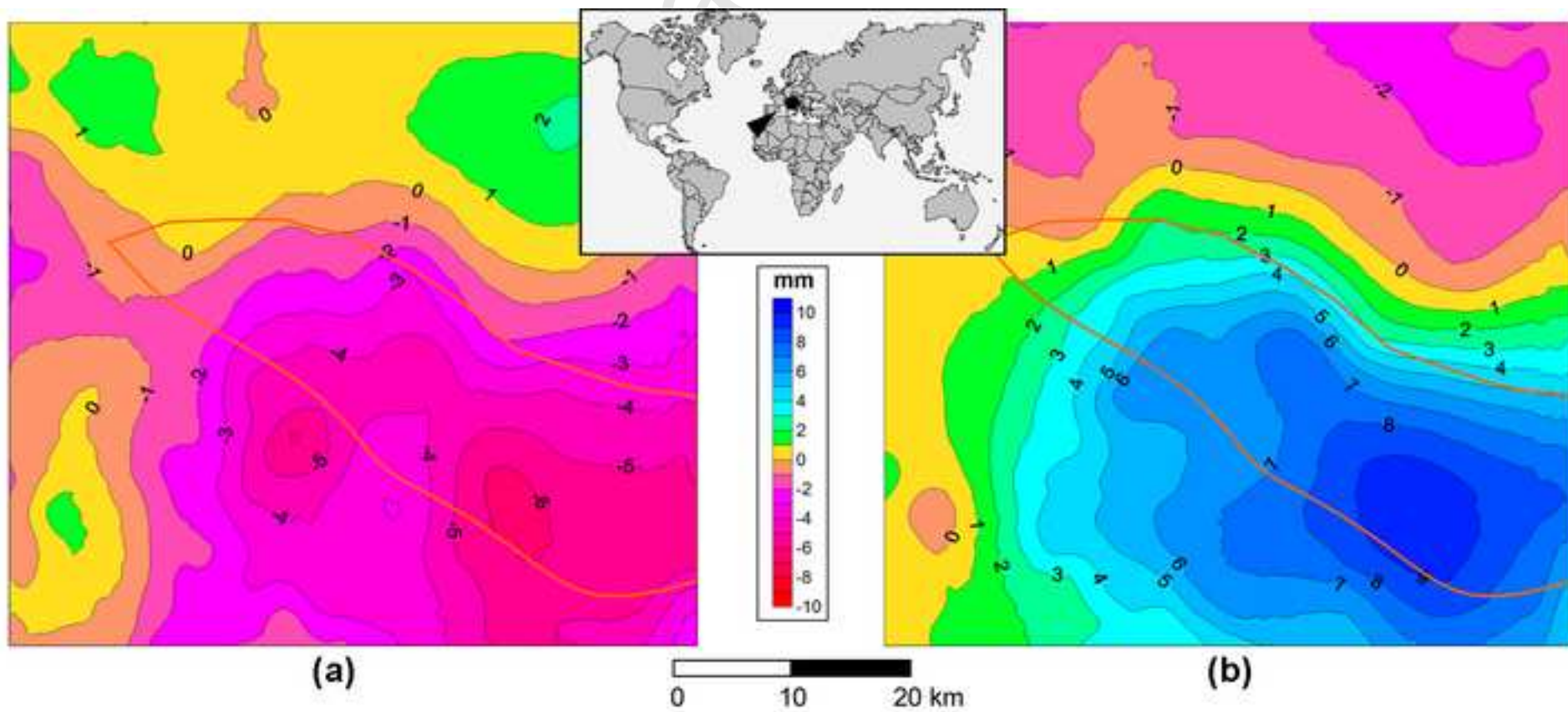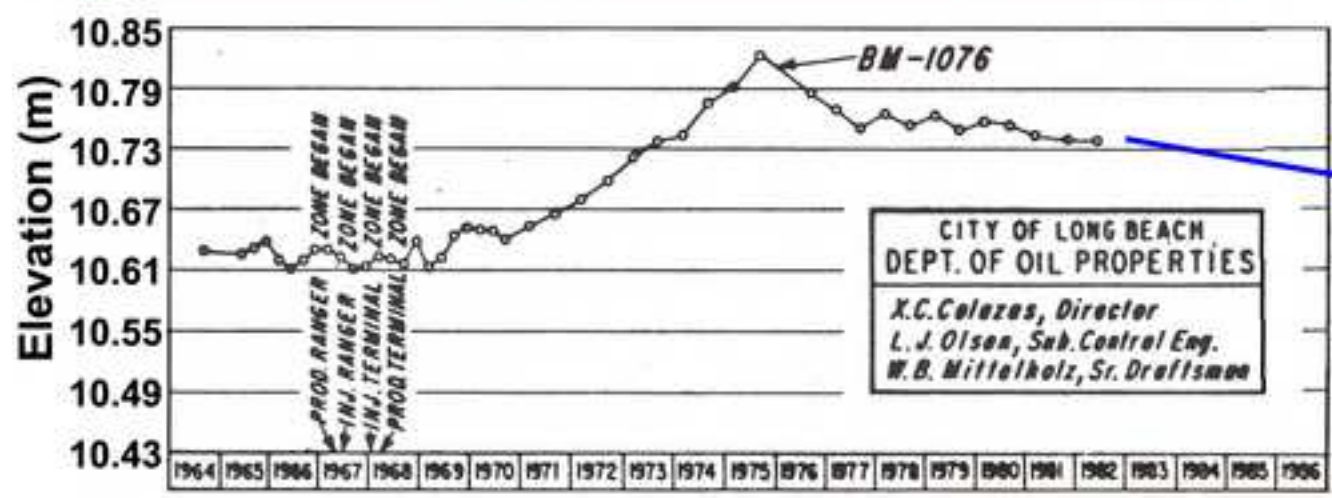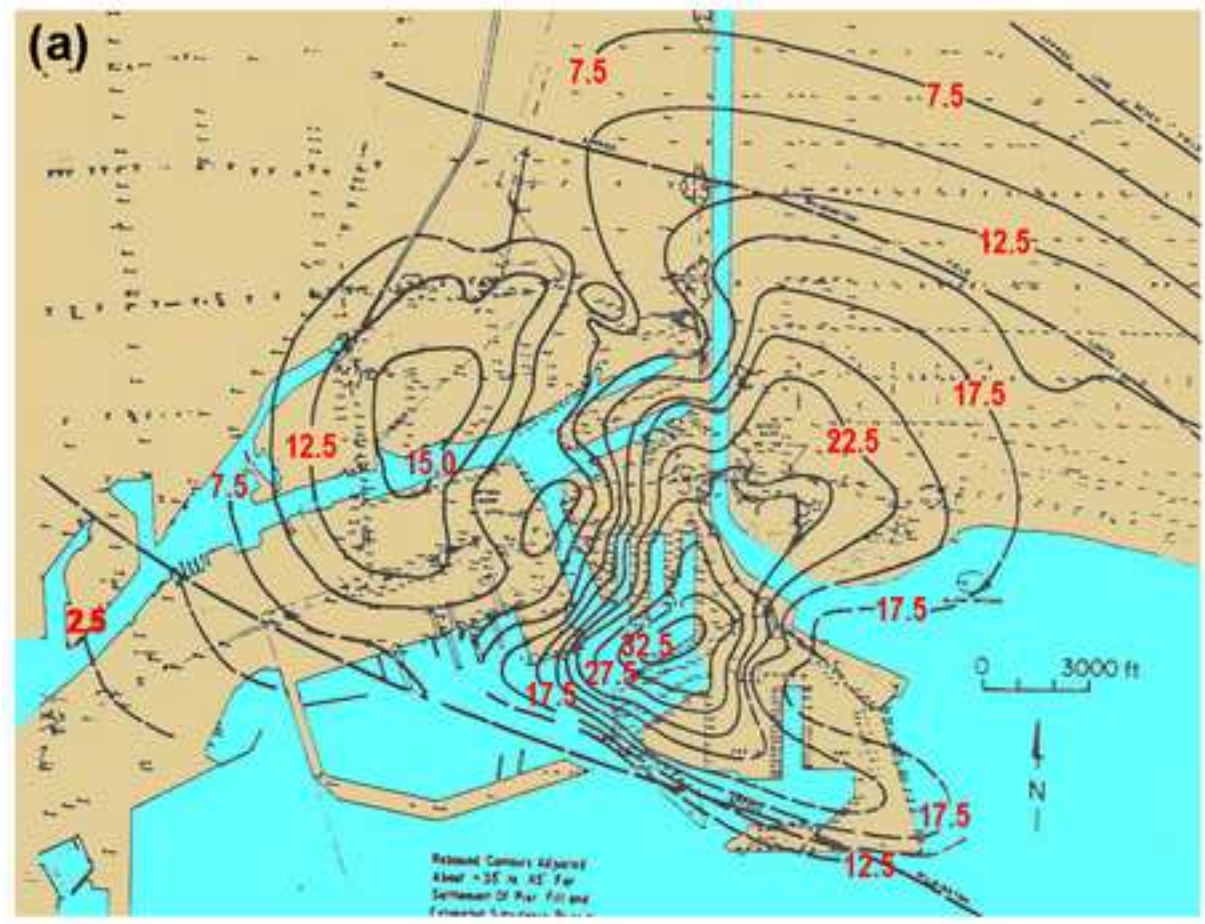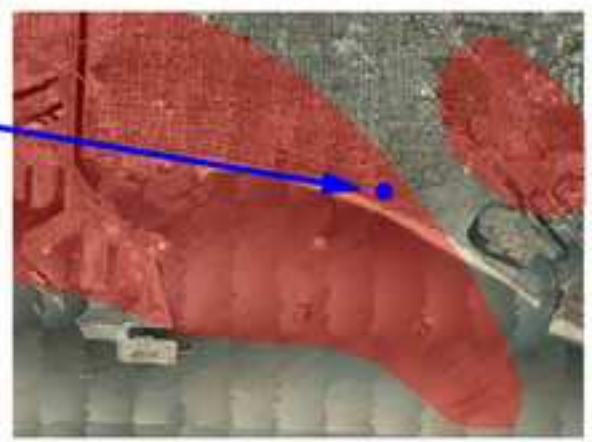
Figure 12
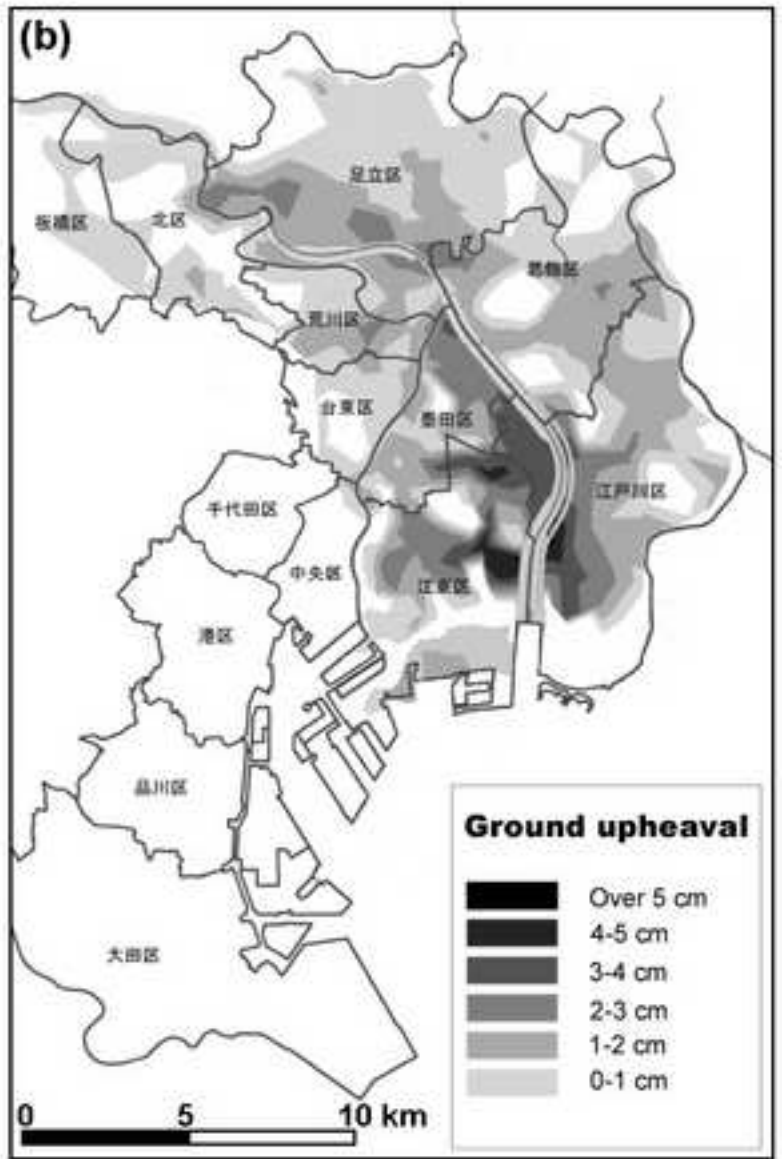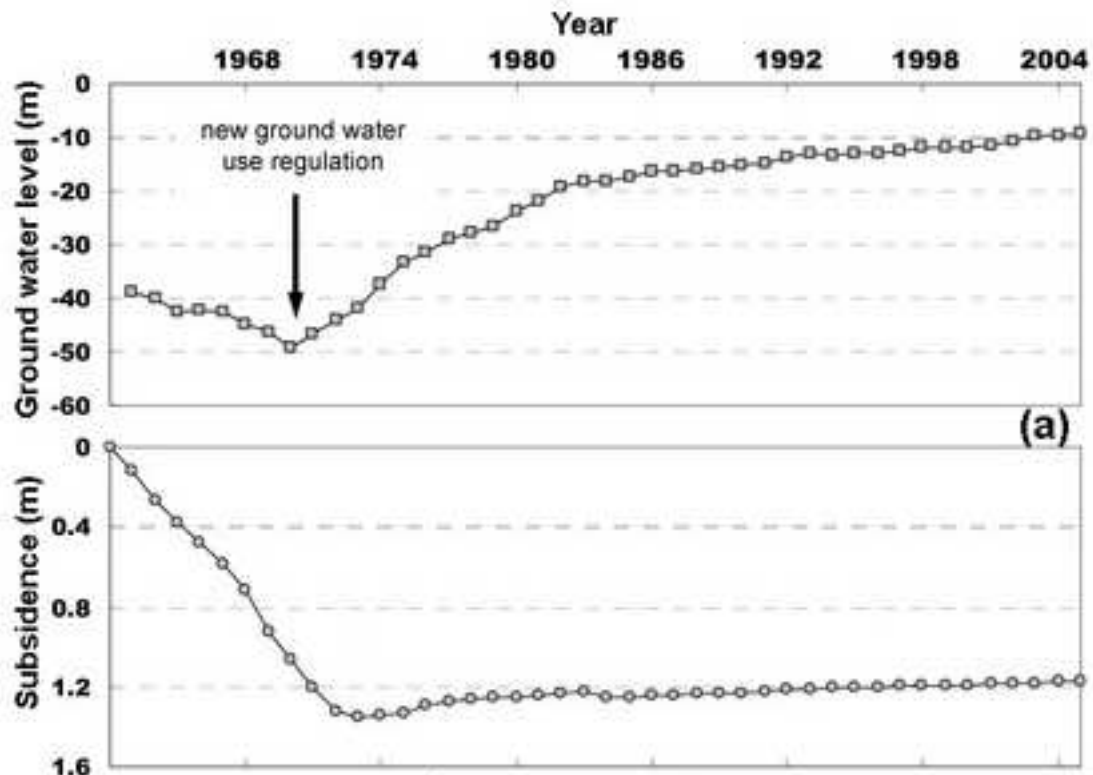
Figure 13

Figure 14
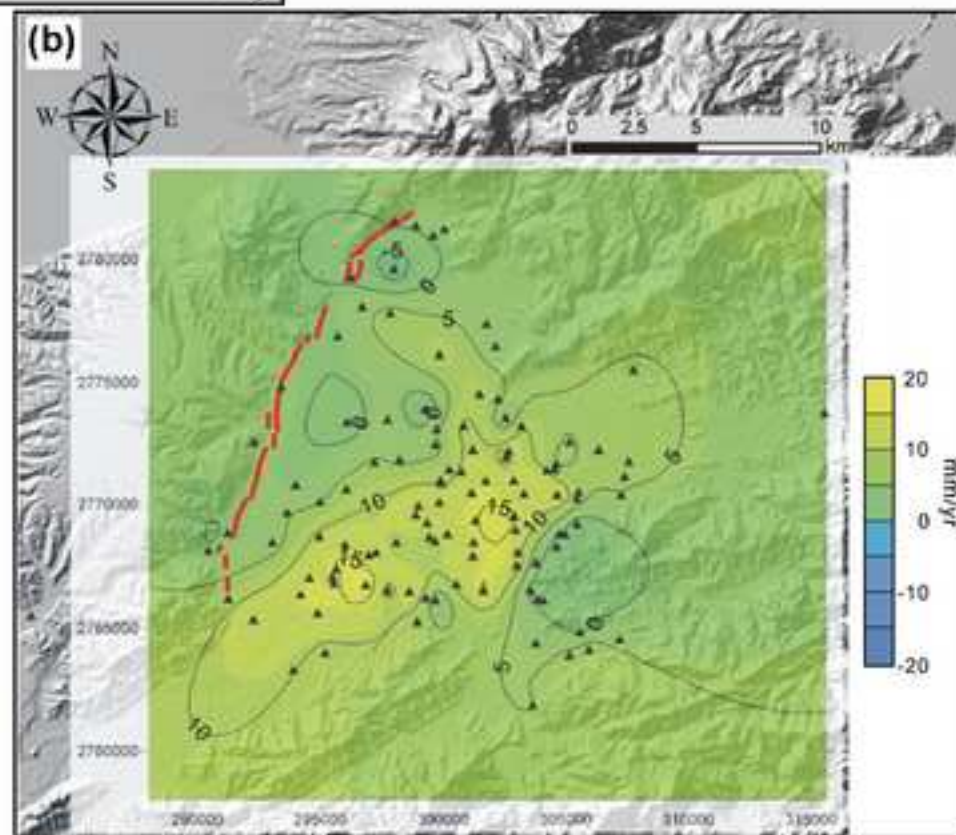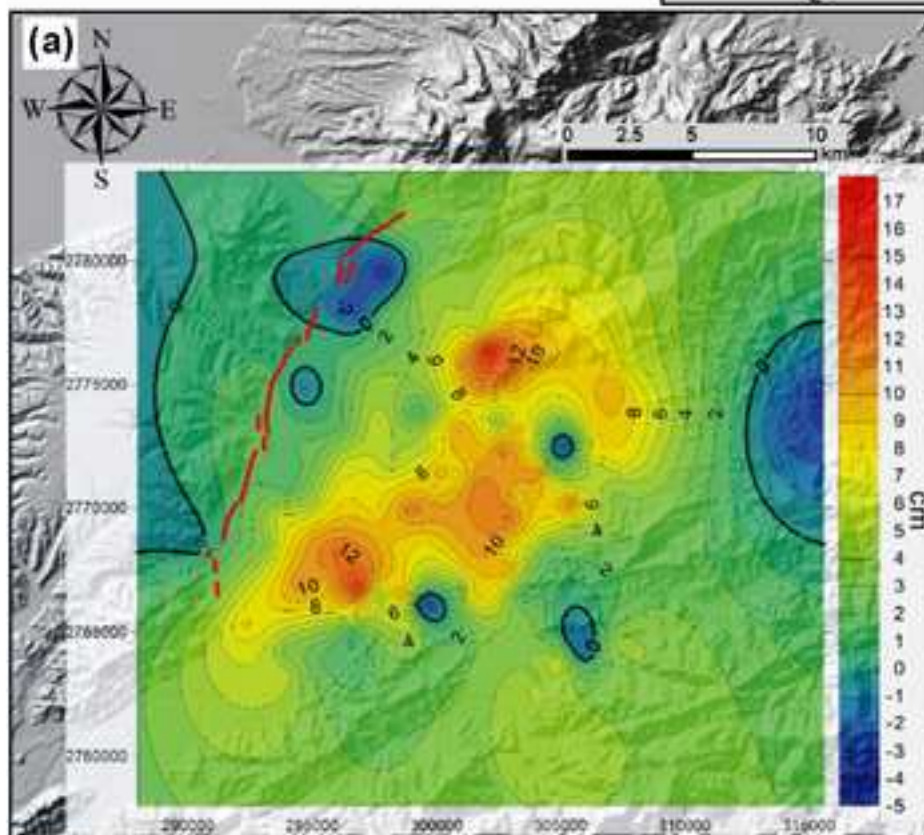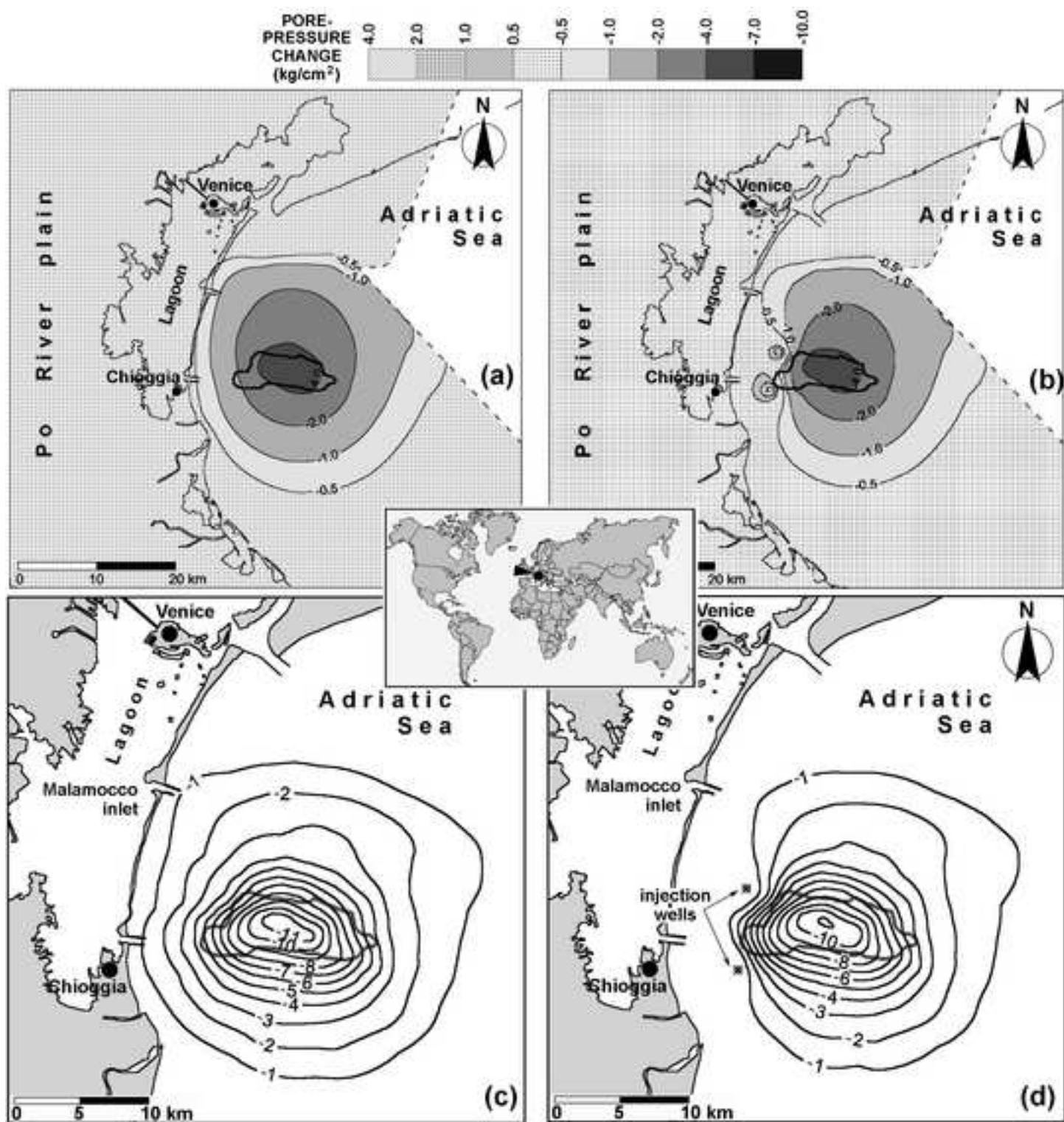
Figure 15
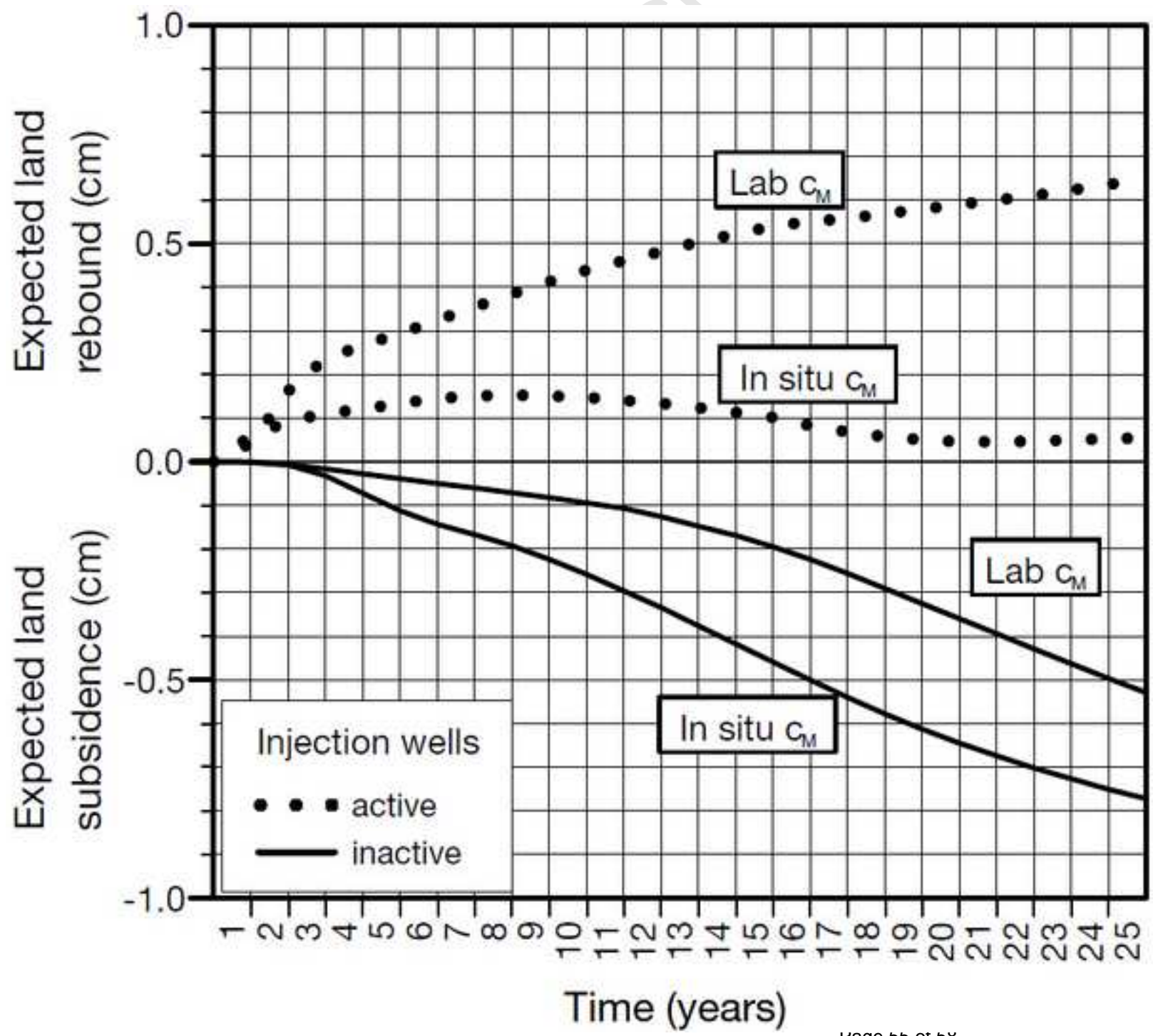
Figure 16

Figure 17

Figure 18

Figure 19